University of Plymouth

A 3D Printed Wearable Exoskeleton for Hand Rehabilitation

I. Parekh

Supervisor: Dr I. Howard

A thesis submitted to the University of Plymouth in partial fulfilment of the requirements for the degree of:

Master of Science, Robotics

September 2019

School of Computing, Electronics, and Mathematics

Faculty of Science and Engineering

Declaration

I confirm that I have read and understood the Plymouth University regulations relating to Assessment Offenses and that I am aware of the possible penalties for any breach of these regulations. I confirm that this is my own independent work.

Candidate's Signature:

Ms Ishita Parekh Date:
23/09/2019

Supervisor's Signature:

Dr Ian Howard I Howard Date: 23/09/2019

Second Supervisor's Signature:

Dr Mario Gianni Date: 23/09/2019

Copyright & Legal Notice

Abstract

Development of hand rehabilitation devices are increasing to assist patients following stroke or accidents. These devices are used to recover motor impairments to assist in the movement and rehabilitation of hand and fingers.

This paper presents the design and implementation of the hand exoskeleton. The exoskeleton device was designed to flex and extend the fingers based on EMG signals received from MYO armband and was actuated using linear actuators (linear servo actuators). The prototype device was designed to be worn on fingers and dorsal side of the hand. This device has transmission mechanism consisting of four bar and five bar linkages actuated by linear servo actuators. The finger exoskeleton was actuated by a sliding motion, mimicking the movement of human finger. EMG signals from the MYO armband device were used to decide the trajectory of the exoskeleton. The entire device was 3d printed, making the device cost effective.

In this thesis, there is discussion of the human hand model and how muscles are affected following a stroke or accidents. Kinematic model of the linkage structure used for transmitting the power and kinematic analysis of the linkage structure for the finger exoskeleton is discussed. The actuation and control mechanism for the exoskeleton and the results are also discussed. Conclusions are also given, and future work is also discussed.

Acknowledgements

I would like to extend my sincere gratitude and thanks to Dr Ian Howard for his guidance, support, accessibility and patience throughout my master's thesis. Without his advice it would not have been possible to complete my master's thesis.

I would also like to extend my sincere thanks and gratitude to Dr Roman Borisyuk, my program advisor for his invaluable support and guidance throughout my MSc program.

I would like to thank Jake Sutton, Senior Robotics Technician, for his invaluable support, guidance, accessibility and patience throughout my MSc project and thesis. Without his guidance and support it would not have been possible to complete my master's project and thesis.

Last but not the least my sincere thanks and deep gratitude goes to my mother and sister. Their never-ending support, encouragement and understanding from far home has always helped to continue and successfully complete my MSc program and thesis.

Contents

List of Figures

List of Tables

List of Abbreviations

Abbreviation	*Meaning*
FES	Functional Electrical Simulation
CIMT	Constraint induced movement therapy
EMG	Electromyograph
HE	Hand Exoskeleton
DIP	Distal Interphalangeal Joint
PIP	Proximal Interphalangeal Joint
MCP	Metacarpophalangeal Joint
DOF	Degree of Freedom
DC	Direct Current
IP	Interphalangeal Joints
FDM	Fused Deposition Modelling
CMC	Carpometacarpal Joint
TCP	Twisted Coil Polymer
SMA	Shape Memory Alloy
PLA	Polyactic Acid
ABS	Acrylonitrile Butadiene Styrene
PC	Polycarbonate
FOS	Factor of Safety
FSM	Finite State Machine

1 INTRODUCTION

Stroke can be defined as the “brain attack”. It usually occurs due to poor blood flow to an area of the brain leading to the death of the brain cells. Due to the death of the brain cells, the functionalities of the brain controlled by that area are lost (for instance speech, limb movement, memory). Post stroke effects basically depend on the area damaged and the amount that area is damaged. For instance, only minor problems like temporary weakness of limbs are caused when people suffer from a small stroke. People may lose their speech ability or might be affected by permanent paralysis due to larger strokes. Stroke is the fourth leading cause of death in the UK. It is the fourth single leading cause of the death in England and wales and it is the third leading cause of death in the Scotland and the Northern Ireland (State of Nation Stroke Statistics, 2018). More than 100,000 strokes occur in the UK every year (that is one in every five minutes). According to the State of Nation Stroke Statistics, Stroke is also the second leading cause of the death worldwide causing around 6.2 million deaths every year causing a death every five seconds. It is also predicted that by 2035, disability in limb movements and deaths will be doubled. In the survey conducted by Stroke Association, there are almost 1.2 million stroke survivors every year and more than three quarters of stroke survivors report limb weakness and difficulty to carry out daily activities. Upper limb motor impairments are most common after a stroke. These post stroke motor impairments lead to loss of functional range of motion of limbs. Hand movements especially flexion and extension of fingers and thumb are largely affected post stroke (Trombly, 1989).

Motor impairments are also caused when people suffer from serious accidents. Accidents also lead to partial or complete loss of movement in limbs. These accidents largely hamper daily life activities.

Rehabilitation forms a key factor in improving strength and movements of limbs affected. Repetitive and task specific exercises are the main elements in rehabilitation of motor weakness. After accidents patients usually undergo physiotherapy sessions to recover motor functionalities of the limbs. Even after stroke, rehabilitation exercises are used to recover limb movements. There are different rehabilitation therapies that are used post stroke, but the main ones include functional electrical simulation (FES), constraint-induced movement therapy (CIMT), robot-based motor therapy and virtual reality. But robot-based therapy is increasing because of its evident advantages over conventional therapies. These advantages include increased repetition of exercises, better motion standardization, patient engagement and increased intensity (O’Dell, Lin & Harrison, 2009).

Rehabilitation of the affected hand is important because it plays a vital role in daily life activities. Different rehabilitation devices have been developed to address the issue of the hand and finger rehabilitation. The state of the art of these rehabilitation devices is discussed in the next chapter. When a stroke occurs, muscle spasticity is experienced in hand (Muscle spasticity – Connections between the hand muscles and the brain gets disrupted resulting into increased stiffness). Even after accidents affecting the hands, in certain cases, hand muscles experience stiffness which disrupts flexion and extension/ adduction and abduction of finger joints.

This thesis focuses on design and implementation of the exoskeleton device for hand rehabilitation. This device would help post-stroke patients and even patients recovering from accidents to perform repetitive exercises and help to restore the motor functionalities of the hand and the fingers.

1.1 Problem Statement

This thesis focuses on following points:

1. 3d designing wearable hand exoskeleton for rehabilitation
2. Controlling the exoskeleton using EMG signals from MYO armband
3. Testing the entire system

1.2 Overview

In this thesis, a design of the hand exoskeleton is discussed. Followed by this, kinematic analysis of the design is provided. Actuation mechanism used to actuate the exoskeleton is also discussed and different actuation mechanisms are compared. Working of MYO armband is explained. Methodology used to extract EMG data from MYO armband is discussed and how this data is used as an input to control the exoskeleton is also discussed. Methods and calculations used to 3d design the exoskeleton are also provided. Two materials used for 3d printing are compared in later sections. High level and low-level design and implementation of a system is also discussed. Results obtained after testing the system are analysed and discussed and conclusions are provided.

2 LITERATURE REVIEW

In this chapter, a literature review of the existing rehabilitation devices for the hand, the kinematic models of the hand implemented by the researchers, control and actuation mechanism suggested by the researchers is discussed. This chapter also discusses about rehabilitation and its different types.

2.1 What is Rehabilitation?

Generally, after accidents people undergo some sort of rehabilitation or therapy to recover from injuries. Post-accident rehabilitation is of two types: physical rehabilitation and cognitive rehabilitation. When limbs are injured during accidents, patients undergo physical rehabilitation. Physical rehabilitation basically refers to a process of regaining muscle strength of the limbs after accidents (AfterTrauma website 2014).

Even when patients that are recovering from stroke undergo physical rehabilitation to recover from motor impairments caused in the limbs. Post-stroke rehabilitation is used to regain the muscle strength of limbs (National Institute of Neurological Disorders and Stroke website 2019).

There are two types of rehabilitation that is used by patients to recover muscle strength in affected limbs. They are:

1. Active Rehabilitation
2. Passive Rehabilitation

2.1.1 Active Rehabilitation

Active rehabilitation therapy or the exercises are usually supposed to be performed by patient themselves. These rehabilitation exercises can be either general exercises or range of motion exercises. These exercises help patients to perform body movements and they also help to strengthen the neural signals (that are used to communicate with human body to perform body movements). This is generally known as cortical plasticity (Saebo Website 2017). When the patient has an impaired muscle movement or an impaired joint after a stroke or an accident, active rehabilitation exercises will help to regain the muscle impairment. This is usually done by retraining the brain signals (neural signals) to communicate with the body via a process called as cortical plasticity (Saebo Website 2017).

Types of exercises include:

Grip-assistive or a task-performing activity which would retrain a neural signal to communicate with the body to regain or strengthen the muscle movements by improving motor impairments. For instance,

In-case of hand movements – trying to grip an object with certain range of motion.

In case of knee injuries - Stretching in and out patients leg that would help to strengthen the neural signals to communicate with the knee and regain the strength.

Other core exercises could also be performed to increase the strength in case of hip and lower back injuries.

2.1.2 Passive Rehabilitation

Rehabilitation exercise is called as passive when an external force is applied to move the muscles. This external force could be another person, or another body part of the same person or an external machine. Passive rehabilitation exercises are generally known as Range of Motion (ROM) exercises. The main purpose of these rehabilitation exercises is to reduce stiffness in the joints of patients, help to stretch the muscles of the limbs affected and also help to increase the range of motion and maintain it (Saebo Website 2017).

Types of exercises include:

In case of fingers affected – flexion and extension of fingers. May also include adduction and abduction of fingers and thumb.

In case of arms or legs affected – stretching the arms or legs and moving them to regain the full range of motion of the arms and legs.

Similar exercises for elbow, wrist or knee impairments with the help of external machine or external support (Saebo Website 2017).

2.1.3 Comparison

Table 1 - Comparison between Active and Passive Rehabilitation Exercise (Drugs.com Website, Merek Manual: Physical Therapy)

Active Rehabilitation Exercise	Passive Rehabilitation Exercise

Helps to build muscle strength	Only keeps joints flexible
Improves fitness of joints and the muscles of patients at the same time	Not able to breakdown muscles with the help of Passive exercises
These exercises are better to improve toning and strength	These exercises only provides sufficient movement to maintain joint flexi

2.2 What is an Exoskeleton device?

Since 80s, many researchers have attempted to replicate the human hand functions and develop a robotic hand. These devices are mainly used in applications like humanoid and industrial robotics, upper-limb prosthetics (device placed in place of the missing hand) and telemanipulation. An exoskeleton device is said to be a special kind of robotic hand. It is also referred as hand exoskeleton (HE) and active hand orthoses. Some examples of active hand orthosis are shown in figs 1, 2 and 3. Figure 1 indicates the wrist driven orthosis for patients with spinal cord injury (Portnova, Mukherjee, Peters, Yamane & Steele, 2018). Figure 2 indicates the tendon driven hand orthosis for stroke patients (Park, Weber, Bishop, Stein & Ciocarlie, 2018). And the hand orthosis indicated in figure 3 was developed by the researchers from institute of robotics, ETH Zurich and Kyushu university. All these orthoses were developed to aid stroke patients with daily life activities.

Figure 1 - Wrist-driven orthosis (Portnova et al., 2018)

Figure 2 - Tendon driven hand orthosis (Park et al., 2018)

Figure 3 - tenoexo: Hand orthosis for therapy and assistance (Lambercy et al., 2017)

2.3 Types of exoskeleton device

As compared to the robotic hands, a hand exoskeleton is an actuated mechanical device which is attached directly to the human hand. Movements between the human hand and the exoskeleton are coupled because of this direct attachment between the two systems. When designing such kind of systems, several factors are considered to enable proper designing.
These factors include:

1. Controlling transmitted forces for safety purposes
2. Synchronising the links of the exoskeleton with the hand.
3. How much force needs to apply to the fingers to perform a given trajectory

Based on the above factors and different functionalities that an exoskeleton is designed for; the hand exoskeleton is divided into three main groups:

1. Rehabilitation HEs
2. Haptic HEs
3. Assistive HEs

2.3.1 Rehabilitation exoskeletons

These are the devices that are designed and developed to perform repetitive exercises and restore motor functions lost by hand after stroke (Yamaura, Matsushita, Kato & Yokoi, 2009).

2.3.2 Haptic devices

Haptic devices are the devices which are not usually considered exoskeleton devices because of its functionalities.
Haptic devices are basically designed for the following functions:

1. Tracking the hand movements of the wearer to control another device
2. Giving a force feedback to the wearer's hand

Tracking the hand movements of the wearer:
Initially, the position sensors are used by the haptic device to measure the position of the human fingers. Then the data gathered by the device is used to control some other

device. Here the other device is called as a slave device, which can be either virtual or real. When the slave device is real then the haptic device is called as a master device. One such master hand developed by researchers Nakagawara, Kajimoto, Kawakami, Tachi & Kawabuchi, 2005 is shown in the figure below. This is a multi-fingered master hand used to control a dexterous slave robot for telexistence. This master hand has an exoskeleton type of mechanism which covers wearer's finger and the hand also has a force feedback which allowed unconstrained movement of the wearer's finger (Nakagawara et al., 2005).

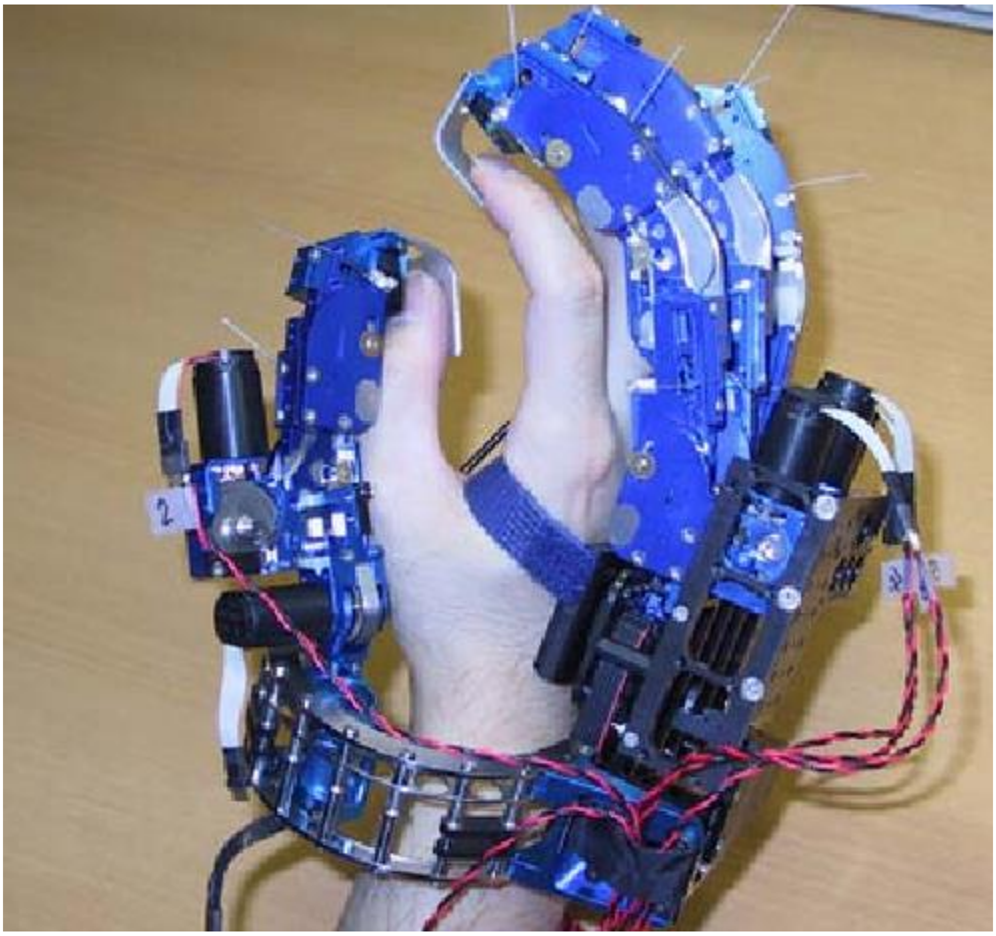

Figure 4 - Encounter-type multi-fingered master hand using circuitous joint (Nakagawara et al., 2005)

Giving a force feedback to the wearer's hand:

Initially, the forces are measured either by the real slave device or by the virtual slave simulator. These measured forces are transferred to the wearer's hand with the help of actuators. This scheme helps the patient feel a natural sense of touch.

2.3.3 Assistive devices

Patients use these kinds of devices to aid them in performing daily life activities, which would be difficult or impossible otherwise. These kinds of devices are also used for rehabilitation purposes. Figure 5 indiactes wearable hand assist device for hand grasping using pneumatic artificial rubber muscle (Sasaki, Noritsugu, Takaiwa and Yamamoto, 2004). It was designed and developed to support patients to perform daily life activities easily and safely.

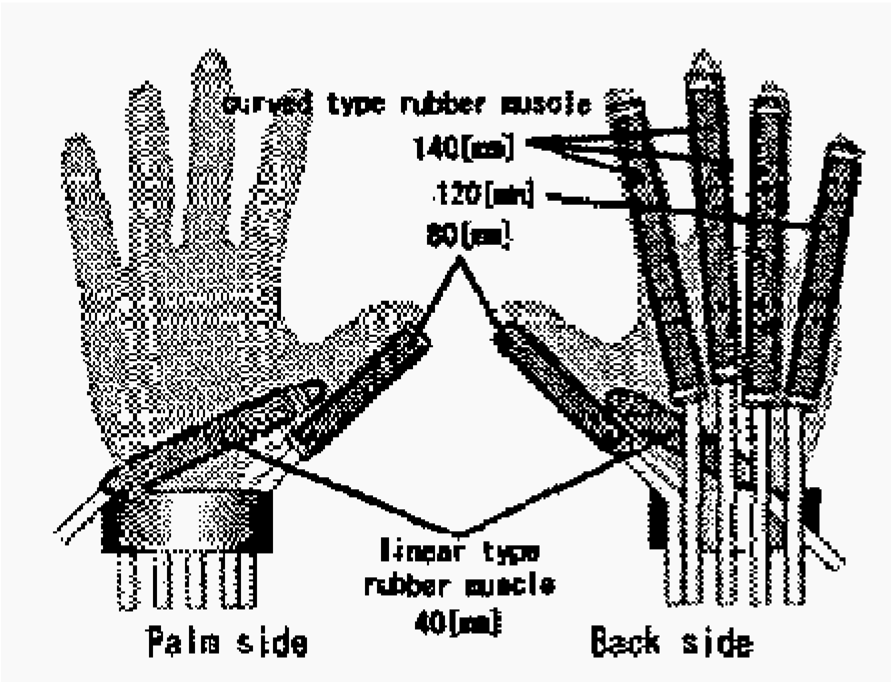

Figure 5 - Power assistance device (Sasaki et al., 2004)

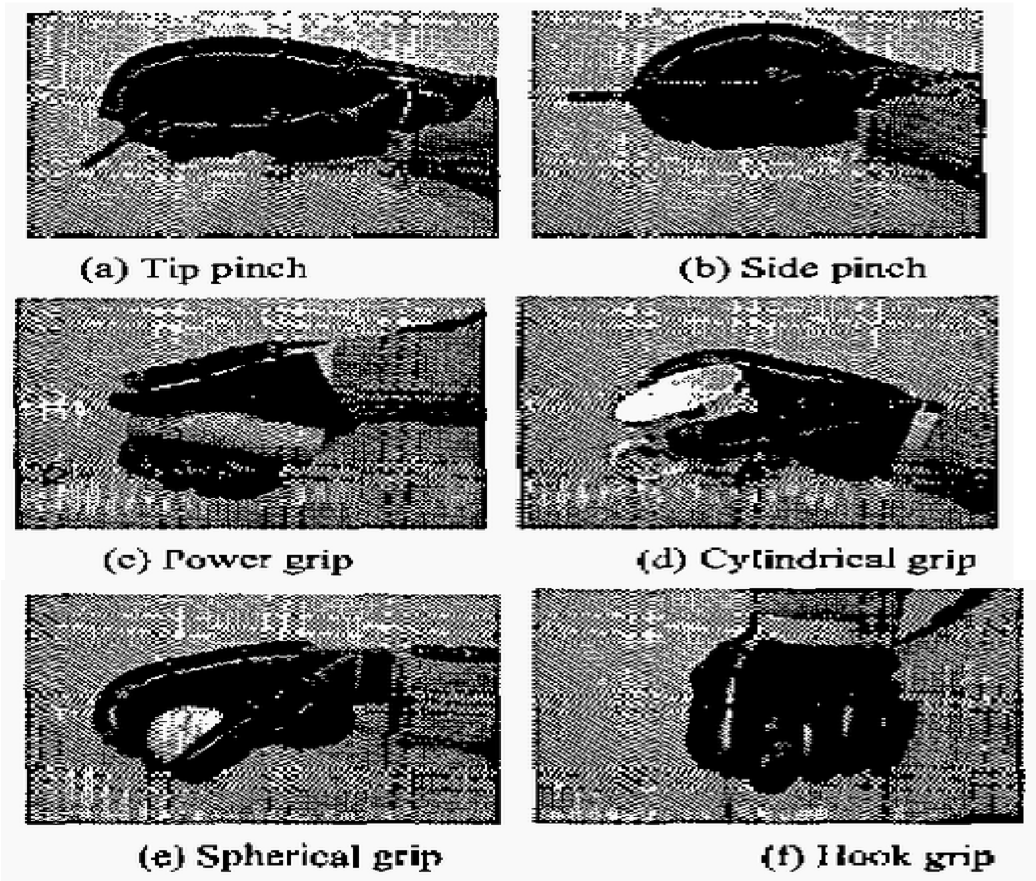

Figure 6 - Scenes of fingers with the assist device (Sasaki et al., 2004)

2.4 Existing Rehabilitation devices

Researchers have proven that repetitive exercises help to restore motor impairments in the upper extremities amongst the patients recovering from stroke (Nef, Reiner and Colombo, 2005). Researchers (Wege and Hommel, 2005) have shown that rehabilitation devices have also helped to improve muscle strength and restore motor impairments caused in the hand after accidents. These researchers have shown that the exoskeletons designed for rehabilitation are more efficient as compared to the manual rehabilitation therapies. Figure 7 shows the exoskeleton device designed and developed by the researchers Wege and Hommel.

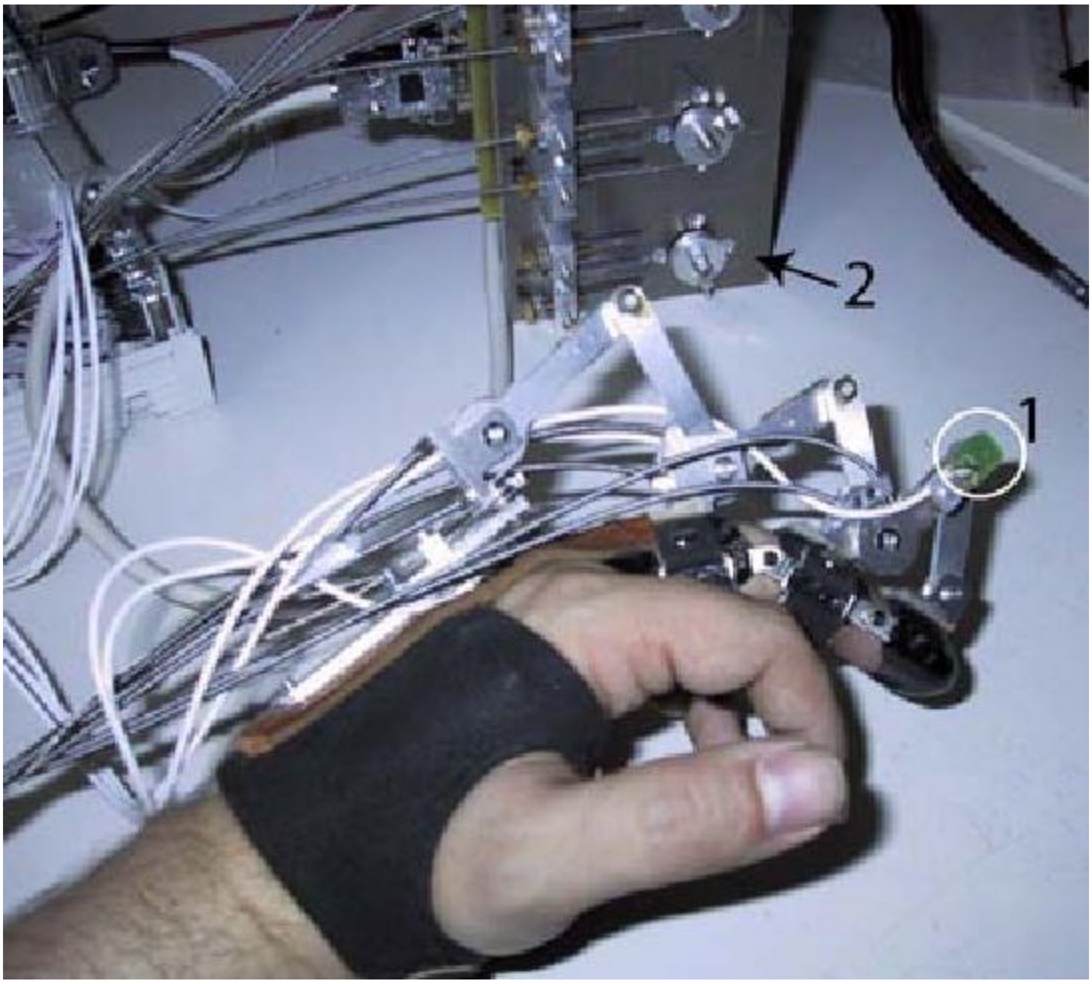

Figure 7 - Exoskeleton for one finger attached to the wearer's hand (Wege et al., 2005)

This exoskeleton was developed to enable bidirectional movement of the exoskeleton. It was designed to support four degrees of freedom for each finger. Each finger has four degrees of freedom and that is flexion or extension at DIP (Distal Interphalangeal joint), PIP (Proximal Interphalangeal joint), MCP (Metacarpophalangeal joint) and adduction or abduction at MCP. This exoskeleton also had palm free of mechanical elements to make the exoskeleton to be light in weight with an intent to make it easy for the patients to wear the exoskeleton.

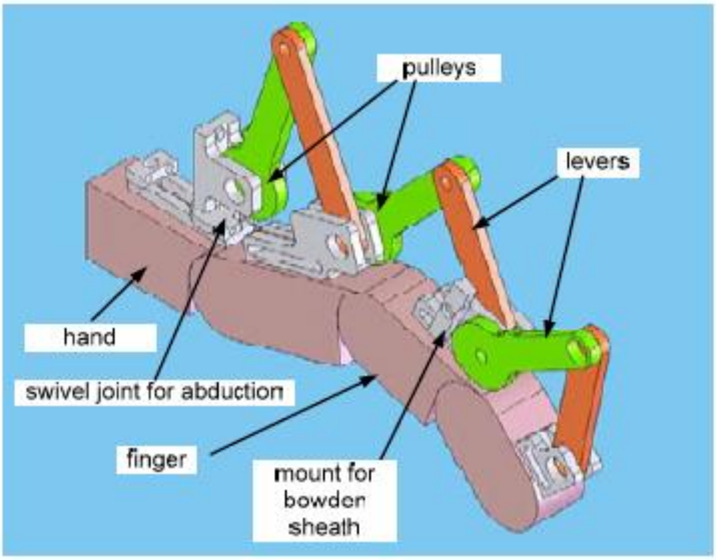

Figure 8 - Exoskeleton design (Wege and Hommel, 2005)

The mechanism that was used to transmit the power to the exoskeleton was the four-bar mechanism. The finger exoskeleton has three four bar mechanisms to actuate the finger exoskeleton. Each of this four-bar mechanism comprises of two human finger links and two external links as shown in the figure.

There are couple of rehabilitation devices that are like the exoskeleton designed by the researchers Wege and Hommel. The University of Tokyo Hand I as shown in the figure 9.

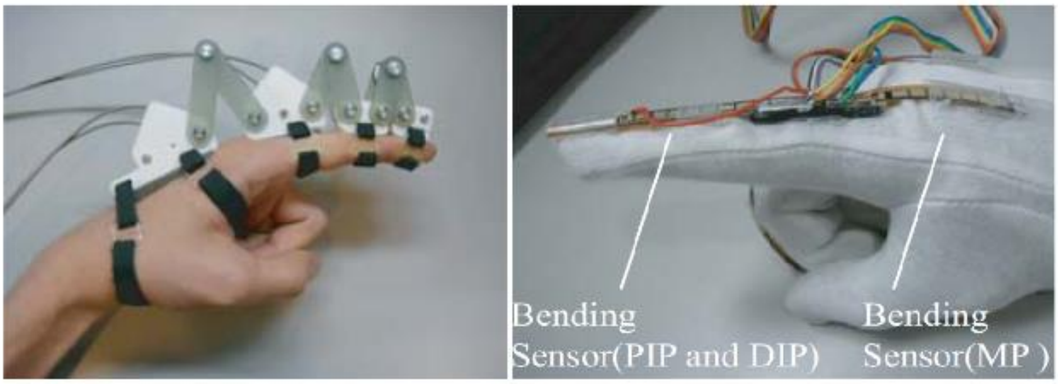

Figure 9 - University of Tokyo Hand I (Yamaura et al., 2009)

Researchers developed this exoskeleton to rehabilitate patients suffering from paralysis. The system comprised two mechanisms. One was exoskeleton device worn on the damaged hand

and the other was the data glove worn on the healthy hand to log finger movements, which is used to control the exoskeleton. The exoskeleton was designed to have 2 DOFs (degrees of freedom), where the movements of the joints PIP and DIP were coupled. The power was transmitted to the finger exoskeleton with the help of linkage mechanism. Three four bar mechanism were used to transmit power to the finger exoskeleton. Each of these four-bar mechanisms comprised of two human finger links and two external links as shown in figure 10a.

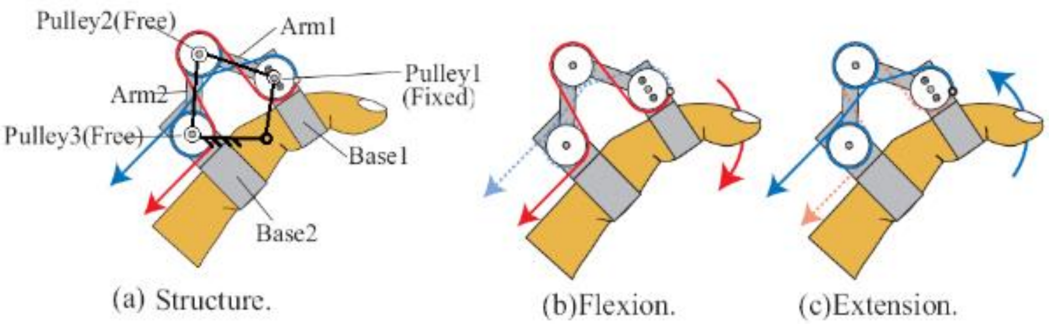

Figure 10 - Power transmitting mechanism for the exoskeleton

The exoskeleton also comprises of four joints of which one is the human joint and three are the external joints. External joints are comprised of two free joints and one fixed joint. The wire-drive mechanism is used as an actuating mechanism to drive this exoskeleton. In this wire-driven or cable-drive mechanism, the fixed pulley is connected to the motor with the help of two wires or cables as shown in the figure 10. The red cable or wire is the flexion cable and the blue cable or wire is the extension cable as shown in the figure 10 b and c. One end of each wire is attached to the pulley’s base and the other end of both the cables are connected to the motor. The actuator contains two servo motor. One servo motor actuates the MCP joint and the other one actuates the coupled joints DIP and PIP of the finger.

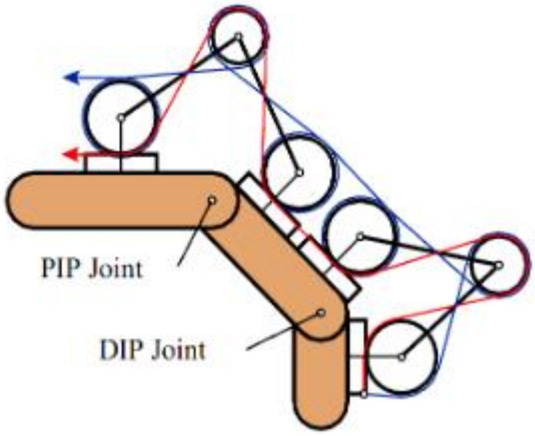

Figure 11 - Coupling between joints PIP and DIP

Another rehabilitation device like the device developed by the researchers from the University of Tokyo is the rehabilitation device developed by the Sabanci University researchers (Ertas, Hocaoglu, Barkana & Patoglu, 2009). This exoskeleton was designed to have 1 DOF. The exoskeleton was actuated by a single DC motor. The power was transmitted to the index finger exoskeleton with the help of mechanical linkages. Mechanical linkage comprised of four bar and five bar linkages connected to each other. This linkage mechanism was connected to all the phalanges of the finger. One DOF was obtained by coupling DIP, PIP and MIP joints of the finger. Figure 12 shows the exoskeleton for the index finger designed by the researchers Ertas et al.

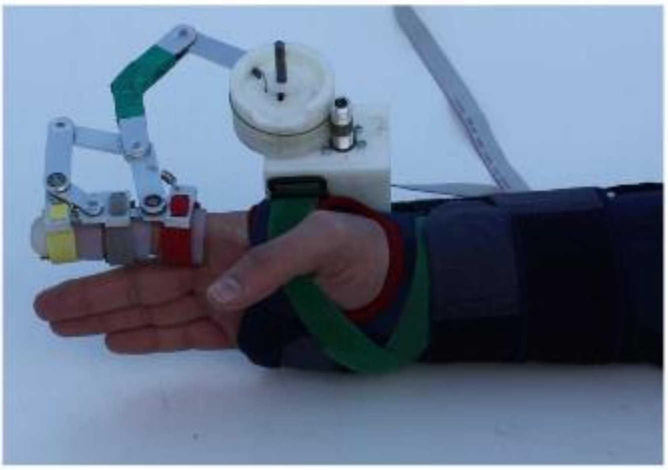

Figure 12 - Index finger exoskeleton by the Sabanci University researchers

Schematic model of the kinematics of the exoskeleton is shown in figure 13.

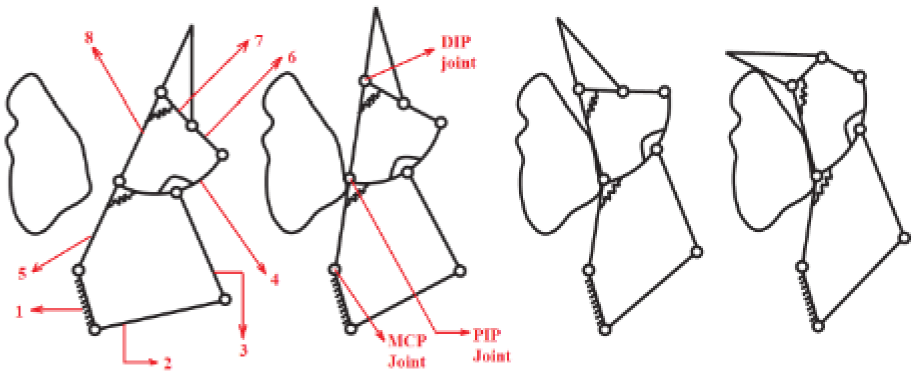

Figure 13 - Kinematics of the exoskeleton for the index finger

As shown in the figure 13, the kinematics of the exoskeleton is nothing but the series of four bar mechanisms (represented by the links 4,6,7 and 8) and five bar mechanisms (represented by the links 1, 2, 3, 4 and 5). As mentioned earlier these mechanisms were coupled together resulting to 1 DOF with the help of two springs.

This exoskeleton device also contained two potentiometers to measure the joint angles. These potentiometers were connected to the exoskeleton joints coinciding with the PIP and DIP joint of the index finger. The exoskeleton was also equipped with optical encoders, which were used to measure the position of the motor axis. The exoskeleton was also equipped with three external force sensors as well. The control mechanism that is used to control the exoskeleton was EMG (Electromyograph sensors).

Another rehabilitation device that used the signals from the EMG sensors to control the movement of the exoskeleton was designed and developed by the researchers from the Pittsburgh University (DiCicco, Lucas & Matsuoka, 2004). This exoskeleton again was deigned to have 2 DOFs. The movements of the PIP and the DIP joint were coupled to get flexion or extension of the finger (representing 1 DOF). Two pneumatic actuators were used to actuate the exoskeleton, one was used to actuate the PIP and DIP joints and one pneumatic actuator was used to actuate MCP joint. Figure 14 shows the exoskeleton design developed by the researchers.

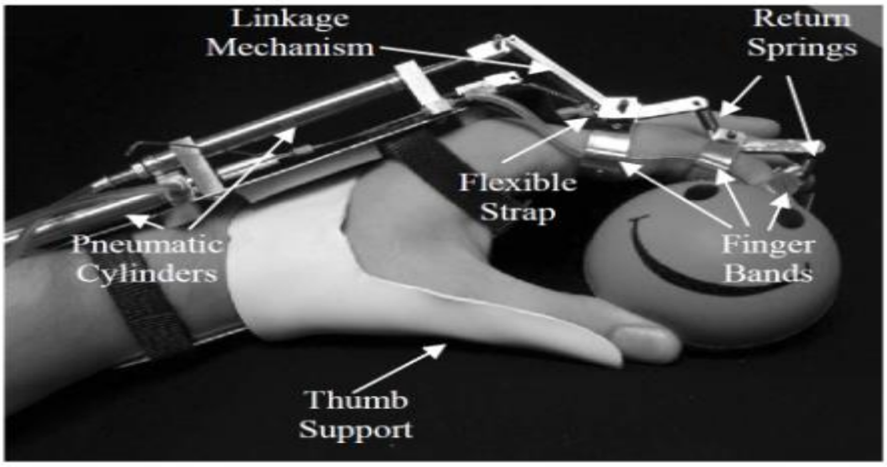

Figure 14 - Hand Exoskeleton

The systems discussed above serve the purpose of rehabilitating the hand recovering from accidents or stroke but each of them has their own advantages and drawbacks. The designed exoskeletons cannot be used anywhere due to its mechanical structure and actuation mechanism. Some of the exoskeletons also targeted to get the natural trajectory of the hand based on the control mechanism used. The exoskeletons that targeted to get natural trajectory of the hand had a complex mechanical structure to be used anywhere by the patients. But the exoskeleton devices that have simple mechanical design has drawbacks with respect to control mechanism.

In this thesis, a hand exoskeleton was designed to have 1 DOF for each finger. Phalangeal joints were coupled to have 1 DOF. Four bar mechanism in series with five bar mechanism was used to transmit the power to the finger exoskeleton and actuate the exoskeleton. The mechanical design of the exoskeleton was completely 3d designed and printed with low cost FDM 3d printers to produce a low-cost exoskeleton. Muscle signals captured from MYO armband were used as a control mechanism for the exoskeleton. The exoskeleton design, control methodology, mechanism of the MYO armband, properties of the material used for 3d printing, high level and low-level design of the entire system are explained in the following sections of the thesis.

3 DESIGN OF HAND EXOSKELETON

3.1 Hand Anatomy

Hand is an organ of the human body that is used for sensing, grasping and communication. The human hand comprises of 29 muscles, 19 joints and 19 bones. Out of 19 bones 14 bones are phalanges which makes up the four fingers and a thumb. The remaining five bones are the metacarpals in the palm of the human hand. Each finger or digits consists of three phalanx bones which are distal phalange, intermediate phalange and proximal phalange. Thumb digit consists of only two phalanx bones which are distal phalanx and proximal phalanx bones. The joints in the hand helps in articulation of the phalanges of fingers and metacarpals of the palm of the hand. Figure 15 indicates the bone structure of the human hand. As shown in the figure 15, carpals are the bones in the wrist of the human hand which helps in articulation of the metacarpal bones (HealthPages Website (2018), www.healthpages.org/anatomy-function/anatomy-hand-wrist).

Each human finger consists of three joints, distal interphalangeal joint (this joint is the closest to the finger tip), proximal interphalangeal joint (this joint is formed between the distal and intermediate phalange) and metacarpophalangeal joint (this joint is formed at the base of the proximal phalange of the finger and thumb). Thumb consists of only two joints one between two phalanges and at the base of the MCP as shown in the figure 15. Flexion and extension are the main movements of the finger at the three rotational joints (indicated by the blue circles) of the finger as shown in the figure 16. These two movements of the fingers are controlled by flexors and extensors. Fingers have two long flexors, a deep flexor and one located superficially. The deep flexor is connected to the distal phalanx and the superficial flexor is connected to the intermediate phalanx (HealthPages Website, www.healthpages.org/anatomy-function/anatomy-hand-wrist).

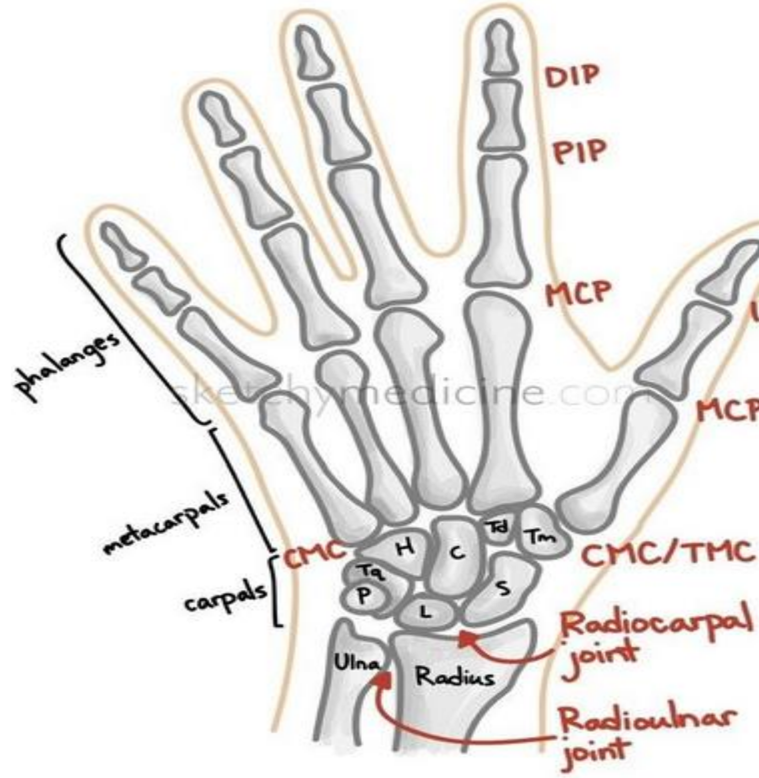

Figure 15 - Bones and joints in the human hand

These flexors connected to the fingers are responsible for actual bending of the finger. The extensors attached to the fingers and the thumb are also located on backside of the forearm. These extensors are responsible for straightening the fingers and thumb. The exoskeleton for rehabilitation was designed based on the flexor extensor mechanism for actuating the finger as shown in the figure 16.

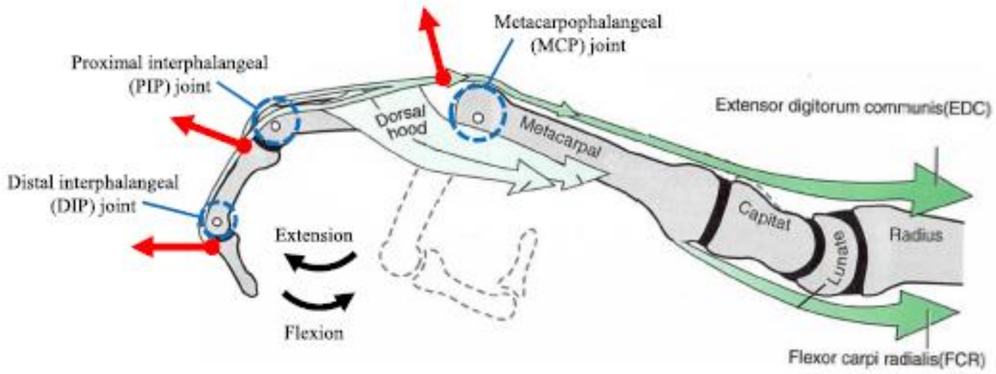

Figure 16 - Movements of the finger and muscles controlling the finger movements

3.2 Mechanical design

The mechanical design of the exoskeleton can be divided into following sections:

1. Design of the finger exoskeleton
2. Design of the dorsal part of the hand

3.2.1 Design of the finger exoskeleton

The finger exoskeleton was designed to have 1 DOF with the three joints of the finger distal interphalangeal joint, proximal interphalangeal joint and metacarpophalangeal joint are coupled together. Three separate exoskeleton parts were designed to cover each phalange of the finger. Three exoskeleton bits were connected together by a pivot joint allowing a smooth movement of the fingers. All the joints of the finger exoskeleton were revolute. The links interconnected the phalanges of the fingers in way that enabled flexion and extension of the finger. Linkage mechanism comprised of a four-bar linkage followed by a five-bar linkage allowing to transmit the power to the exoskeleton. Adduction and Abduction is another degree of freedom for the finger, but for the design of this exoskeleton this degree of freedom was not considered and only flexion and extension of the phalangeal joints was considered.
The mechanical design of the finger exoskeleton is shown in the figure below.

Figure 17 - Finger Exoskeleton

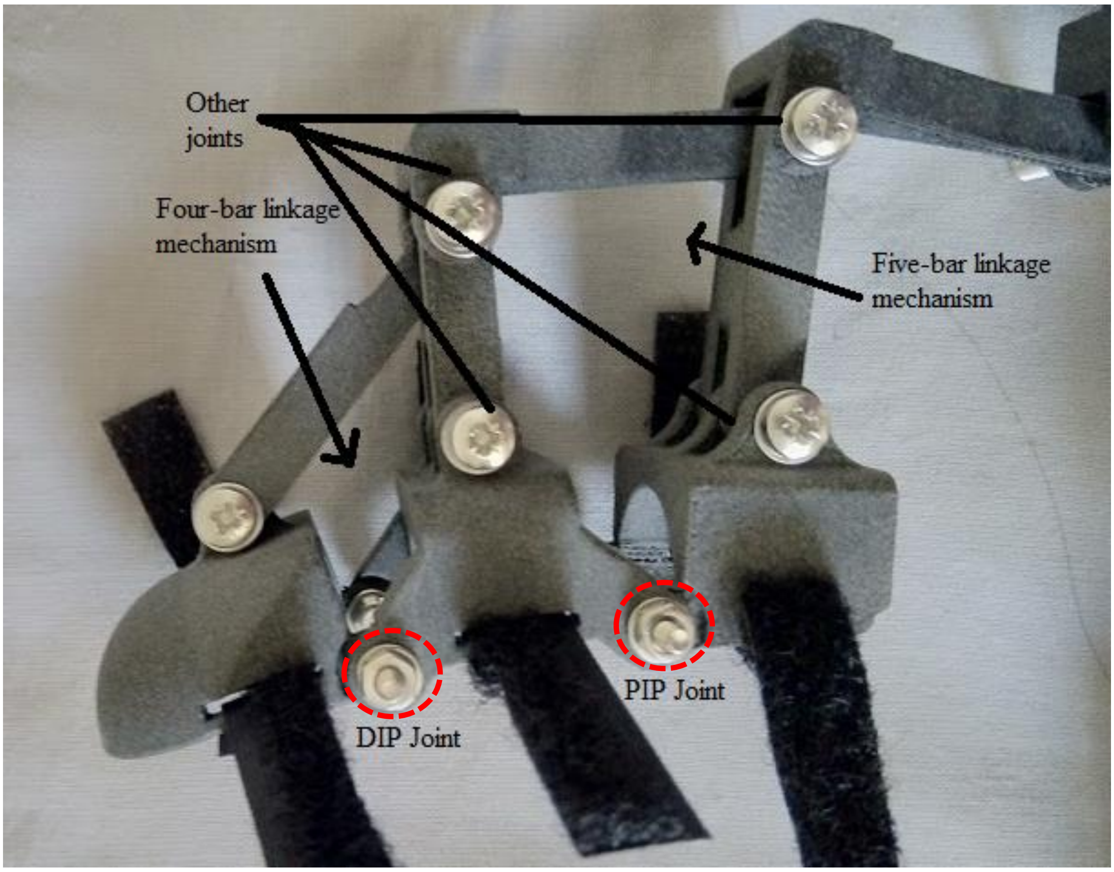

Figure 18 - Parts of the finger exoskeleton

Each finger exoskeleton was designed to have a four-bar linkage followed by a five-bar linkage as a linkage mechanism to transmit the power. As shown in the figure 18, there are two pivot joints in the exoskeleton that are synchronized with the distal interphalangeal joint and intermediate phalangeal joint of the finger. These pivot joints are indicated by the red dashed circles in the figure 18. The link lengths and joint angles at which the links are connected were calculated by performing kinematic analysis of the link lengths of the four bar and five bar linkages and the measurements of the finger used to 3d design the exoskeleton structure for the finger. Kinematic analysis of the kinematic model of the finger exoskeleton and four bar and five bar linkages is discussed in the next section.

The proposed design structure of the finger exoskeleton is as shown in the figure 18.

The proposed structure was designed to be on top of the finger as shown in the figure 18. The reason for this design was to avoid interference between the fingers, to avoid linkages or other structures to interfere with adjacent fingers.

3.2.2 Design of the dorsal part of the hand

The mechanical design of the exoskeleton for the dorsal part of the hand is shown in the figure 19.

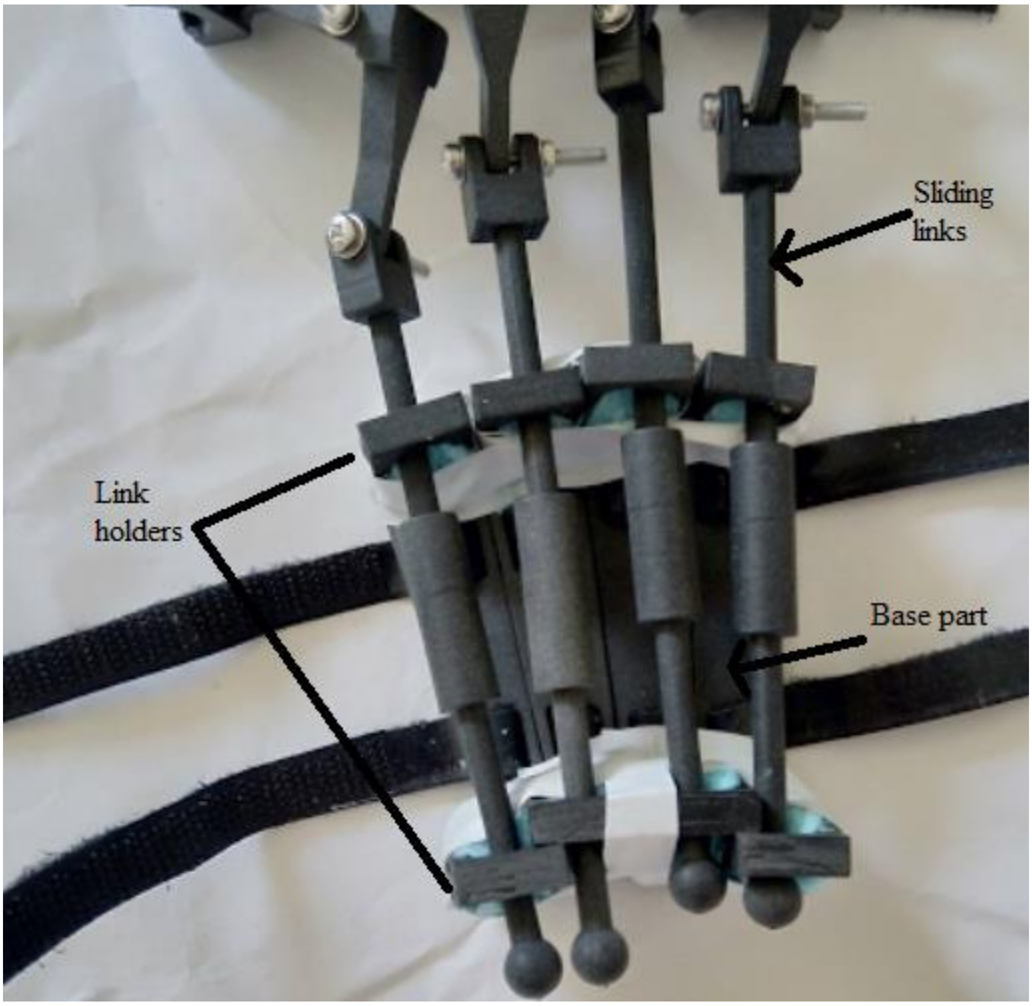

Figure 19 - Dorsal part of the hand exoskeleton

All the mechanical parts were designed to be attached on the dorsal side, based on how the extensor muscles are placed, to make the entire design of the system to be compact. Design of this module to connect the finger exoskeleton to the actuator was a challenging task. As rehabilitation device was supposed to be designed and developed to be used by patients recovering after stroke and accidents, it was necessary to ensure perfect fitting of device on the hand. The device should not be too tight, as it would cause difficulty and discomfort to the patients. On the other hand, if the design of device is loose or too loose, then the power transmission to the finger exoskeleton would be hampered and effective motion of the exoskeleton would also be affected.

The prototype of the entire device, the finger exoskeleton and structure connecting the finger exoskeleton to the actuator is shown in the figure 20.

Figure 20 - Prototype of the hand exoskeleton

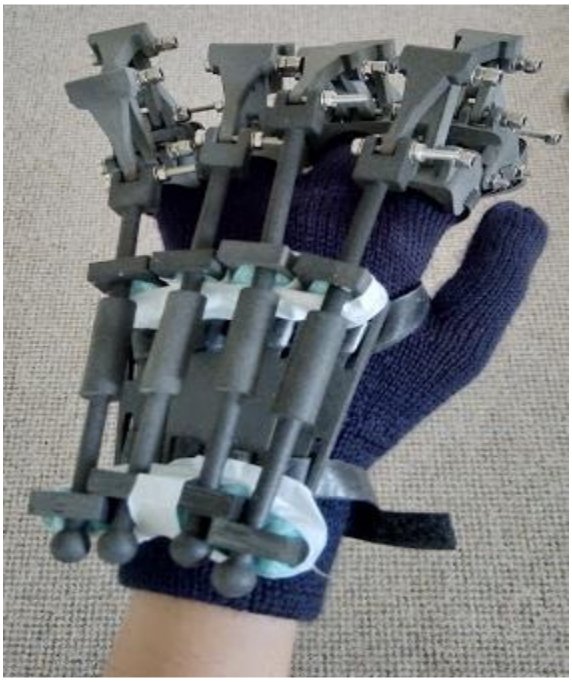

Figure 21 - Other side of the hand exoskeleton

As it is evident from the figure 21, the metacarpal segment is composed of the base plate. Four separate base plates were designed based on the measurement of the metacarpal segment of the hand. The four plates were attached together with Velcro straps and were connected to the glove as shown in the figure. On top of the base plate, sliding mechanism was attached. The sliding mechanism's one end was connected to the base link of the finger exoskeleton and the other end was connected to the actuator. The design employed was the simplest to ensure development of a lightweight exoskeleton that could be used by the patients anywhere they want.

3.2.3 Power transmission mechanism

If actuators are placed near to the fingers or on the dorsal side of the metacarpal segment, then the load on the patients' hand might increase, causing discomfort to the patients. For this reason, actuators are placed away from the hand on the forearm. To transmit the power from the actuators to the finger exoskeleton, so that finger exoskeleton could have the effective motion, linkage mechanism was used in the finger exoskeleton and linear sliding mechanism was used. This can be seen in the figure 19, 20 and 21.

4 KINEMATIC ANALYSIS OF THE FINGER EXOSKELETON

This chapter discusses the kinematic analysis of the kinematic model of the finger exoskeleton. The performance of the exoskeleton depends on the length of the link of the exoskeleton. With the proper link length, a highly efficient hand exoskeleton design is possible, otherwise, improper link lengths may result into high torque resistance. Thus, kinematic analysis of the kinematic model of the finger exoskeleton was performed to get a proper link length.

4.1 Kinematic Analysis of the finger exoskeleton

The proposed linkage structure for the finger exoskeleton can be divided into a four-bar linkage followed by a five-bar linkage. A four-bar linkage has two human finger linkages and two external links, and a five-bar linkage has three external links and two human finger links. The kinematic model of the proposed linkage structure is shown in figure 22 (Kinematics Wikipedia, 2019).

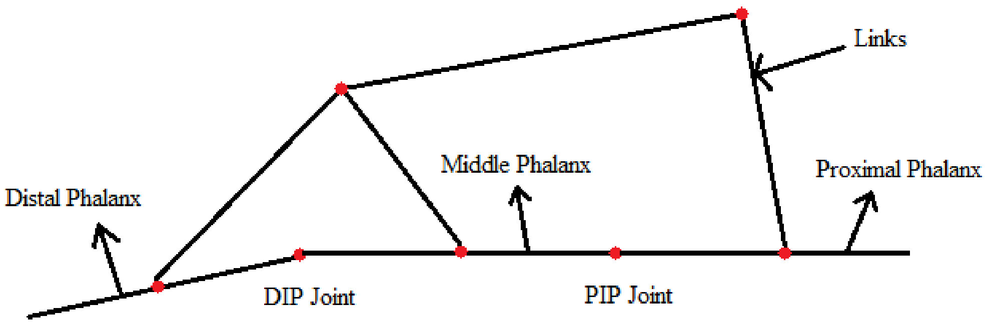

Figure 22 - Kinematic model of the proposed linkage structure

As shown in the figure, red dots indicate the joints and other are the links. The divided kinematic model is shown in the figure 23. The numbers inside each linkage indicate the number of links in the respective linkage.

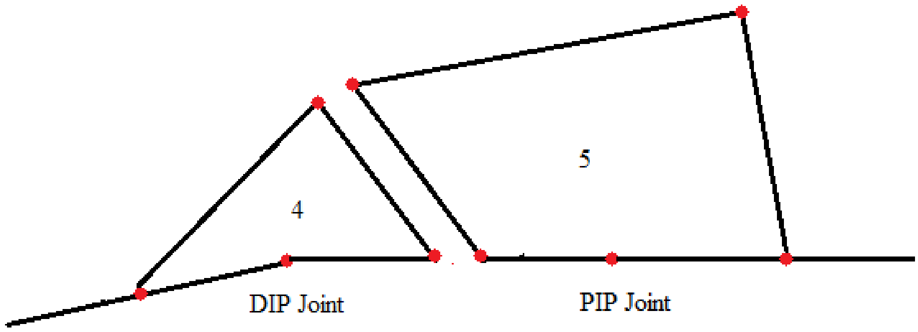

Figure 23 - Divided kinematic model of the linkage structure

As seen in the figure 24, length variables are defined for kinematic analysis of the proposed linkage structure. Figure 25 shows the angles of DIP, PIP and MCP joints. It can also be seen from the figures 24 and 25, the x axis of the kinematic model was set parallel to the dorsal part of the hand.

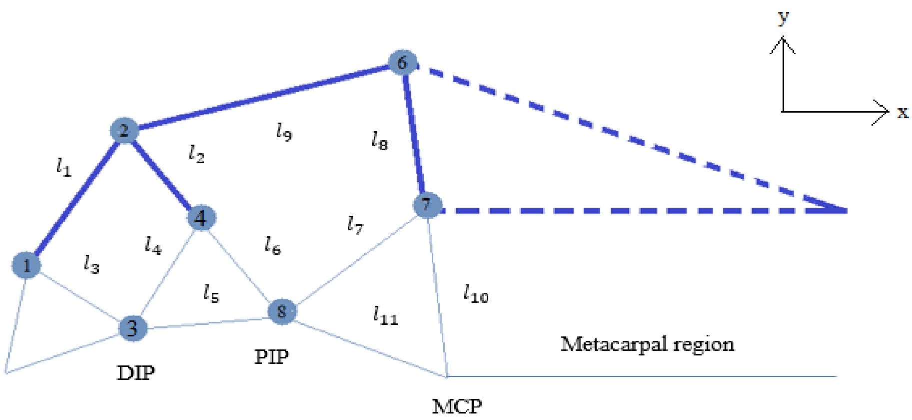

Figure 24 - Length variables of the linkages

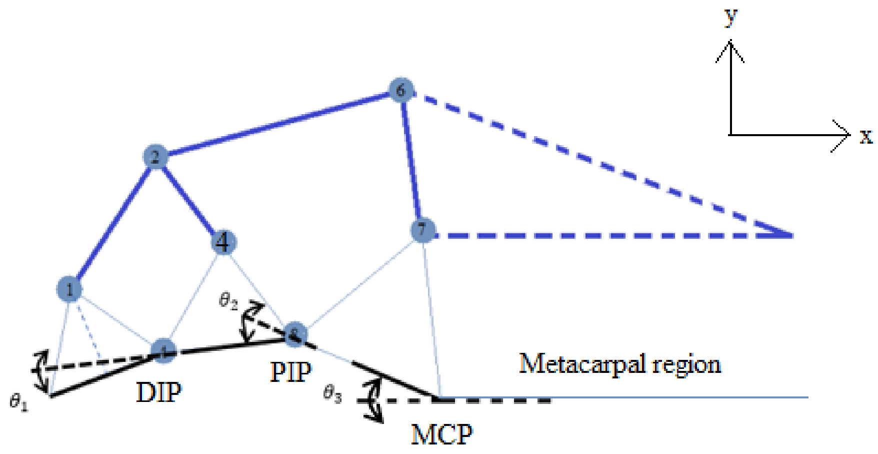

Figure 25 - Finger joint angles

As the exoskeleton was used for repetitive exercises and not for performing activities like grasping, pinch, key grip so functional range of motion was not considered. The normal range of motion was considered, and it was compared with the range of motion that each joint of the finger reached with the proposed linkage structure. The predefined parameters and other parameters that were used for kinematic analysis is as listed in table 1.

Table 2 - Parameters for kinematic Analysis

Link lengths		*l*
Position	DIP Joint	Point 4
	PIP Joint	Point 8
	MCP Joint	
Range of finger joint angles	DIP (degrees)	Flexion: 0 to 80 degrees Extension: 80 to 0 degrees
	PIP (degrees)	Flexion: 0 to 120 degrees Extension: 120 to 0 degrees
	MCP (degrees)	Flexion: 0 to 90 degrees

		Extension: 0 to 30 degrees

4.1.1 Determining the position of joints in linkage structure

The joint angle values ($\theta_1, \theta_2, \theta_3$) were used to determine the position of the finger joints DIP, PIP (at point 4 and 8 respectively). The positions of the joints at points 1, 3 and 7 were calculated automatically as these were the joints on the phalanges of the finger. The remaining joint positions were determined by doing an analysis of the four-bar and five-bar linkages.

4.1.2 Analysis of four-bar linkage

The schematic of the four-bar linkage is shown in the figure below

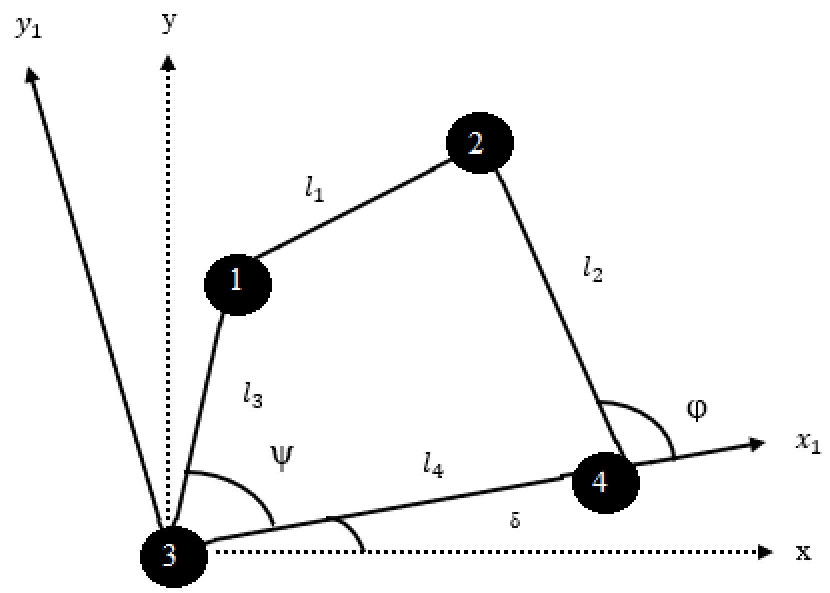

Figure 26 - Schematic of the four-bar linkage

The four-bar linkage as shown in the figure is a planar RRRR linkage. The degree of freedom for the linkage structure is given by Grubler-Kutzbach's criterion. It is defined by the following question:

$$DOF = \lambda(N - J - 1) + \sum_{i=1}^{J} F_i \qquad \ldots (1)$$

Where, N - total number of links (including base link)

J – total number of joints (connecting only two links)

F_i – DOF at the ith joint

For a planar 4-bar RRRR linkage, N = 4, J = 4, λ = 3 (for planar manipulators), resulting into 1 DOF. As the linkage has 1 DOF it has one input angle and one output angle. As shown in the figure 26, ψ is an angle included between links l_3 and l_4 (input angle) and φ is the output angle. The lengths of the links in the linkage structure are defined by the set of parameters $\{l_i\}_1^4$. The general equation relating the input and output angles of the linkage can be expressed in the non-dimensional form and it is given as follows:

$$k_1 + k_2 \cos\varphi - k_3 \cos\psi - \cos\psi \cos\varphi - \sin\psi \sin\varphi = 0 \quad \ldots (2)$$

The above equation is called as Freudenstein equation and parameters k_1, k_2 *and* k_3 are known as Freudenstein parameters.

For the linkage structure shown in figure 26, Freudenstein parameters are given as,

$$k_1 = \frac{l_4^2 + l_3^2 - l_1^2 + l_2^2}{2 l_3 l_2} \quad \ldots (3)$$

$$k_2 = \frac{l_4}{l_3} \quad \ldots (4)$$

$$k_3 = \frac{l_4}{l_2} \quad \ldots (5)$$

This equation relates the link lengths, input and output angles.

As shown in the figure 26, the plane $x_1 - y_1$ is tilted from the plane x - y by angle δ. The angle δ is calculated by using joint position at points 3 and 4, which is investigated before. The input angle ψ can also be given by using cosine rule, given as follows:

$$\psi = \arccos\left(\frac{l_3^2 + l_4^2 - \left\|\overrightarrow{P_1} - \overrightarrow{P_4}\right\|^2}{2 l_3 l_4}\right) \quad \ldots (6)$$

As shown in the figure 25 and 26, joint at point 2 in the linkage structure, is the joint of the links of the distal and intermediate phalanx. Calculating the position of the joint at point 2 will also give the correct estimation of the link lengths in the linkage structure shown in the figure 26.

Given that ψ is an input angle of the linkage structure shown in figure 26, position of the joint at point 2 is calculated as follows (McCarthy, 1999):

$$\left(\overrightarrow{P_1} - \overrightarrow{P_2}\right).\left(\overrightarrow{P_1} - \overrightarrow{P_2}\right) - l_1^2 = 0 \quad \ldots (7)$$

Where, $\overrightarrow{P_1} = l_3 T(\psi)$ and $\overrightarrow{P_2} = l_4 [1\ 0]^T + l_2 T(\varphi)$ in the $x_1 - y_1$ plane of the linkage structure.

In general form the input-output equation is rewritten as:

$$A(\psi)\cos\varphi - B(\psi)\sin\varphi + C(\psi) = 0 \quad \dots (8)$$

Where,

$$A(\psi) = 2l_2l_4 - 2l_2l_3\cos\psi \quad \dots (9)$$

$$B(\psi) = 2l_2l_3\sin\psi \quad \dots (10)$$

$$C(\psi) = l_3^2 + l_2^2 + l_4^2 - l_1^2 - 2l_3l_4\cos\psi \quad \dots (11)$$

Then, the output angle φ, is determined based on previous equations and the input angle ψ of the linkage structure. And the output angle φ is given by following equation:

$$\varphi = arctan\left(\frac{B(\psi)}{A(\psi)}\right) \pm arccos\left(-\frac{C(\psi)}{\sqrt{A(\psi)^2+B(\psi)^2}}\right) \quad \dots (12)$$

Thus, in terms of position of joint at point 4, the output angle of the linkage structure, from above equations, the position of the joint at point 2 can be given as:

$$\overrightarrow{P_2} = \overrightarrow{P_4} + l_2T(\delta + \varphi) \quad \dots (13)$$

Thus, all the joint positions and link lengths were investigated for the linkage structure shown in figure 26 with the help of four bar linkage analysis (Bai and Angeles, 2008).

4.1.3 Analysis of five-bar linkage

As shown in the figure 22 and 23, kinematic model of the linkage structure consists of a five-bar linkage followed by the four-bar linkage. Five-bar linkage has 3 external links, l_2, l_8 and l_9 and two human links l_6 and l_7 as shown in the figure 24.

The schematic of the five-bar linkage is shown in the figure below:

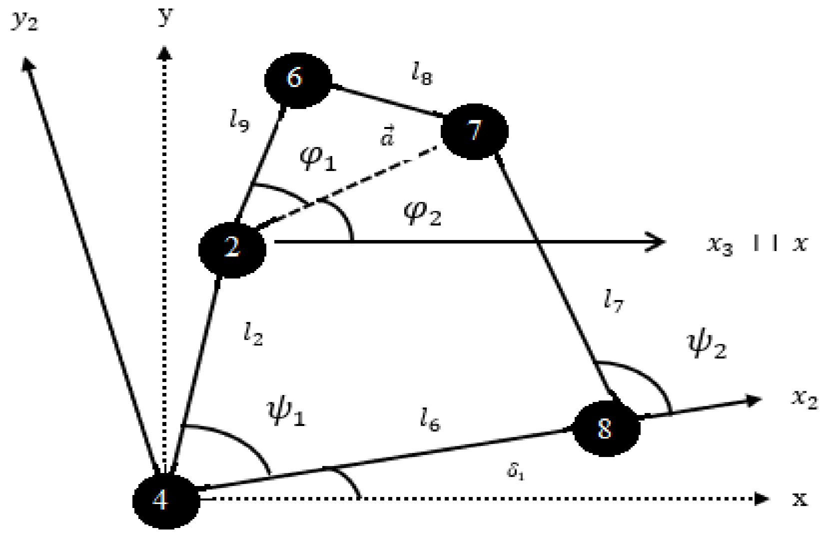

Figure 27 - Schematic of the five-bar linkage

As shown in the figure 27, the linkage structure is planar five bar mechanism. The linkage structure, as shown in the figure 24, 25 and 27, has five links and five joints. The resulting degree of freedom for planar five-bar mechanism with N = 5 and J = 5 was 2 degrees of freedom. As the five-bar planar linkage mechanism has 2 DOFs, two input angles are required to analyse the linkage structure and to find the position of the joints in the linkage structure. As shown in the figure 27, ψ_1 *and* ψ_2 are the input angles for the linkage structure. It can also be seen that, $x_2 - y_2$ plane is titled with respect to the normal x – y plane by an angle δ_1. The angle δ_1 is calculated by the positions of the joints at points 4 and 8 as shown in the figure 27.

The joint positions 4 and 7 were already investigated in the previous section (It can be automatically calculated as these are attached on the parts present on the distal and intermediate phalanx).

The input angles ψ_1 *and* ψ_2 can be calculated using cosine rule, same as calculating the input angle ψ for the four-bar linkage structure.

As shown in the figure 25 and 27, joint at point 6 in the linkage structure, is the joint of the links of the intermediate and proximal phalanx. Calculating the position of the joint at point 6 will also give the correct estimation of the link lengths in the linkage structure shown in the figure 27.

Position of the joint at point 6 is given as:

$$\overrightarrow{P_6} = \overrightarrow{P_2} + l_9 T(\varphi_1 + \varphi_2) \quad \ldots (14)$$

To calculate φ_1 *and* φ_2, the vector $\vec{a}$ connecting the joint at point 7 to the joint at point 2 is calculated.

Vector $\vec{a}$ is calculated as follows:

$$a = \overrightarrow{P_7} - \overrightarrow{P_2}$$

$$= \overrightarrow{l_6} + \overrightarrow{l_7} - \overrightarrow{l_2}$$

$$= l_6 T(\delta_1) + l_7 T(\delta_1 + \psi_2) - l_2 T(\delta_1 + \psi_1) \quad \ldots (15)$$

With the calculated vector a, angle φ_1 is calculated as follows:

$$\varphi_1 = arccos\left(\frac{l_9^2 + \|a\|^2 - l_8^2}{2l_9\|a\|}\right) \quad \ldots (16)$$

Angle φ_2 can also be calculated by making use of vector a as follows:

$$\varphi_2 = arccos\left(\frac{a \, . \, [1\ 0]^T}{\|a\|}\right) \quad \ldots (17)$$

Thus, the joint position at point 2 was determined by calculating vector a and angles φ_1 *and* φ_2 (Hassaan, 2015).

Thus, all the joint positions and link lengths were investigated for four-bar and five-bar linkage structure of the finger exoskeleton.

The table showing link lengths and joint angles of the linkage structure are as follows:

Table 3 - Link lengths of the linkage structure

Links	Dimensions (mm)
l_1	40.879
l_2	26.13
l_8	33.419
l_9	39.32

The joint angles between the linkages are as follows

Table 4 - Joint angles of the linkage structure

Joint positions	Angle dimensions (degrees)
At joint position 2	44.2
At joint position 6	155.7

5 ACTUATION MECHANISM

In this chapter, the actuation mechanism used to control the hand exoskeleton is discussed. Different available actuation mechanisms are also discussed in this chapter and the proposed actuation mechanism for controlling the hand exoskeleton is compared with respect to advantages and disadvantages with other available actuation mechanisms.

5.1 What is an actuator?

An actuator is a machine component which is used to move or control the system. It is often denoted as a “mover”. To control or move the system to which actuator is connected, it needs two parameters: control signal and the source of energy. The control signal used for the actuator, is usually a low energy signal which can be either electric current or voltage, pneumatic pressure, hydraulic pressure or in some cases it can be a manual power as well. The primary source of energy for an actuator can be either pneumatic or hydraulic pressure and electric current. When an actuator receives the control signal, it converts the energy of the signal to mechanical motion. Based on these two parameters there are different kinds of actuation mechanisms. These actuators are designed to serve purpose for several applications and each actuator comes with its own advantages and disadvantages (Actuator Wikipedia, 2019).
The different types of actuators are as follows:

1. Hydraulic actuator
2. Electric actuator
3. Pneumatic actuator
4. Twisted and coiled polymer (TCP)
5. Magnetic or thermal actuator
6. Mechanical actuator
7. 3d printed soft actuators

5.1.1 Hydraulic actuator

Hydraulic actuator is a type of linear actuator. It consists a hollow cylinder and a piston within the hollow cylinder. An external pump filled with incompressible fluid is used to move the piston inside the hollow cylinder. Movement of piston can result into three resultant mechanical motions: linear motion, rotatory motion or oscillatory motion (Machine design Website, 2016).

A basic hydraulic actuator is shown in the figure below:

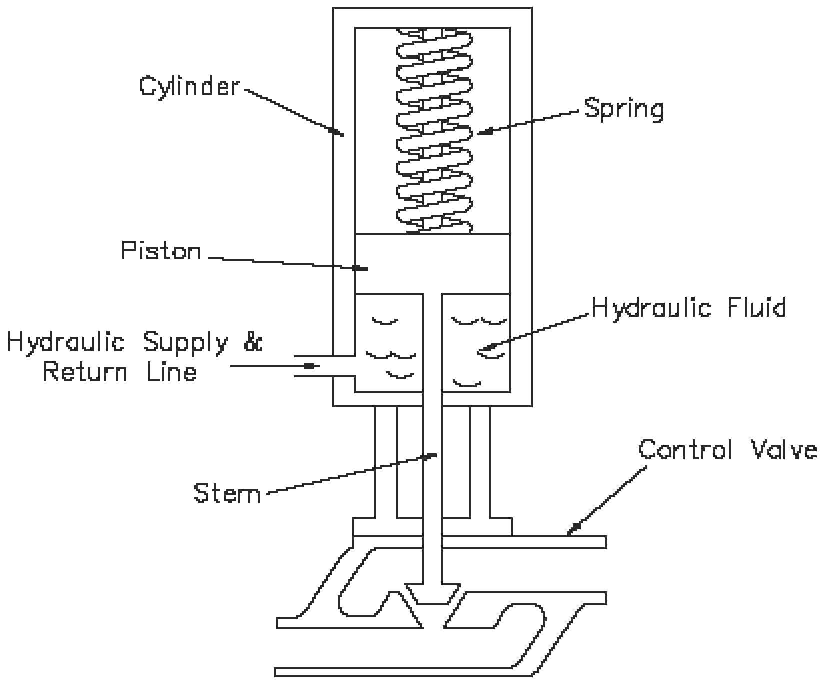

Figure 28 - Basic hydraulic actuator

5.1.2 Pneumatic actuator

Pneumatic actuator is also another type of linear actuator. The construction and working of pneumatic actuator is like the hydraulic actuator but pneumatic actuator uses external compressor instead of incompressible fluid to move the piston inside the cylinder. With increase in the pressure, the hollow cylinder moves along the axis of the piston, resulting into linear force (Machine design Website, 2016 and Tech FAQ Website, 2018). Two methods are used to bring the piston back to its original position:

Spring-back force

Supplying fluid to the other end of the piston

A basic pneumatic actuator design is shown in the figure below:

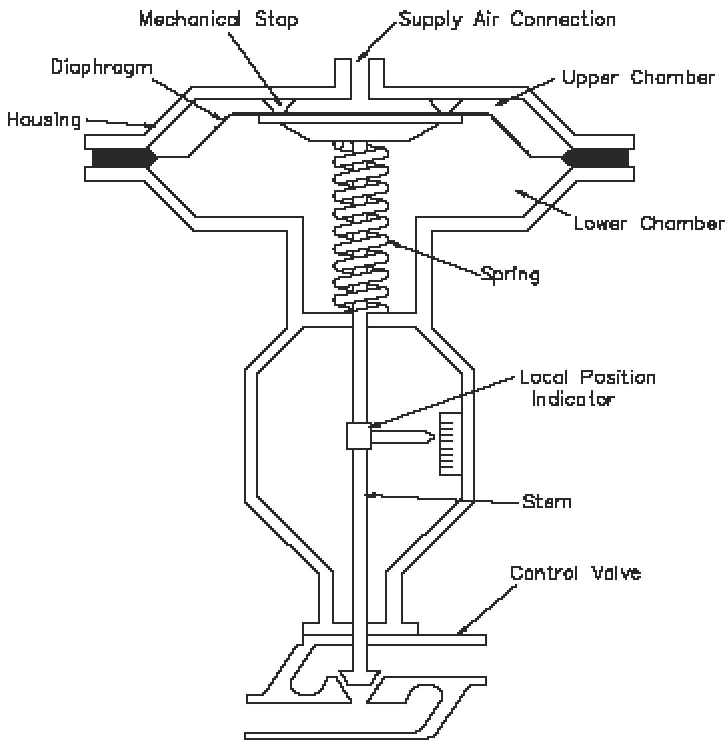

Figure 29 - Basic pneumatic actuator

5.1.3 Electric actuator

An electric actuator is powered by the motor to convert electrical energy into mechanical torque. This electrical energy is used to control the movement of the mechanical system (Actuator Wikipedia, 2019). The basic electric linear actuator is shown in the figure below:

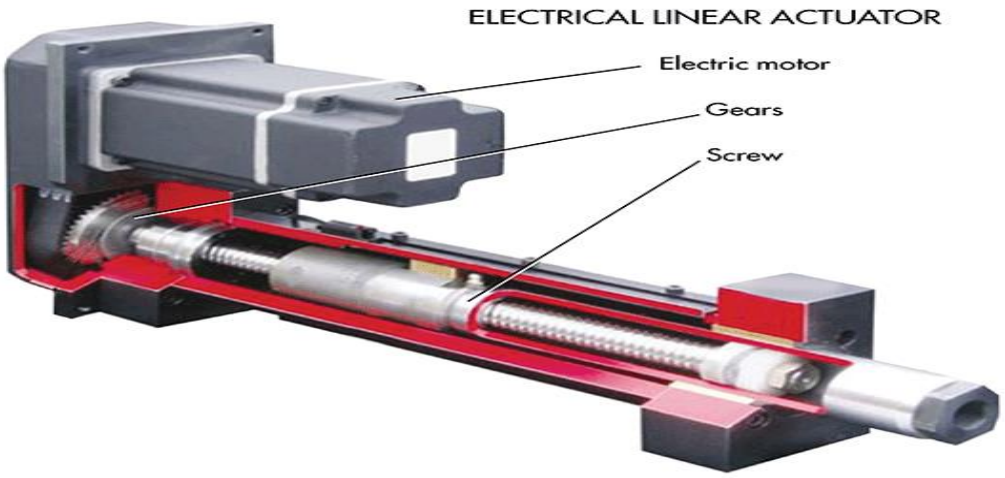

Figure 30 - Basic electric actuator

As shown in the figure 30, the motor that drives the actuator is the part of the actuator instead of being separate as in the case of hydraulic or pneumatic actuator.

5.1.4 Twisted and coiled polymer (TCP)

TCP is a coiled polymer which uses electric motor for actuating the mechanical system. The coiled polymer has a spring like structure, and it is made up from silver coated nylon or other conductance material like gold. Initially, the electrical energy is converted to the thermal energy, this is the result of Joule heating (Also known as ohmic or resistive heating). Joule heating leads to increase in the temperature, which leads to polymer contraction which in turn results in the contraction or relaxation of the actuator (Actuator Wikipedia, 2019).

The following figure shows TCP muscle and its fabrication process:

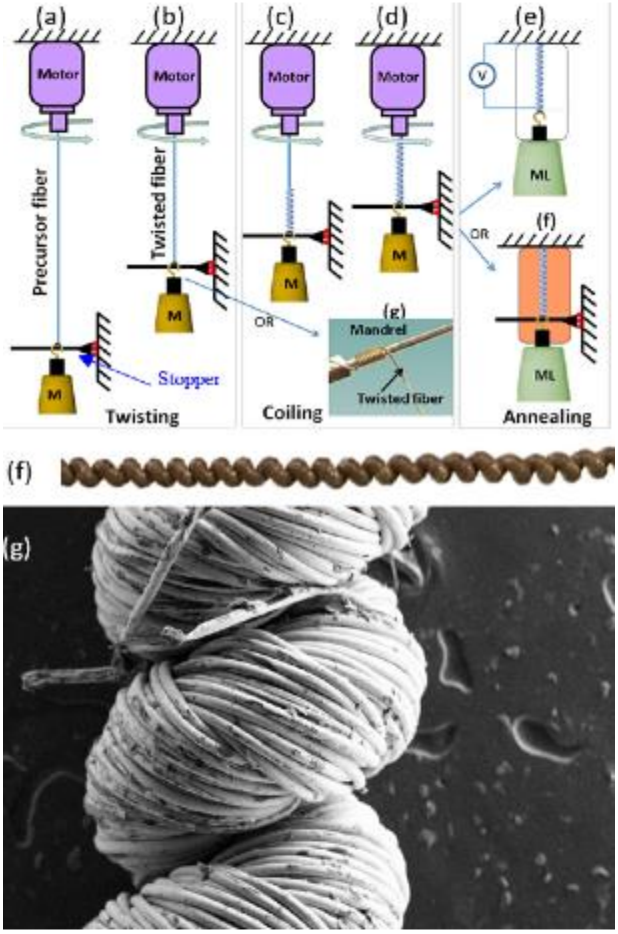

Figure 31 - TCP muscle and its fabrication process

5.1.5 Thermal or magnetic actuator

These kinds of actuator make use of magnetic or thermal energy to actuate the mechanical system. Examples of such actuator includes shape memory materials like shape memory alloys (SMAs). Shape Memory alloys are used in many robotic applications because of the alloy's features (Actuator Wikipedia, 2019).

5.1.6 Mechanical actuators

These are the kinds of actuators which are basically used to convert one type of motion into another type of motion. For instance, converting rotary motion to linear motion. This type of actuation is a result of combination of different structural components like pulleys, gears, chains, rails. An instance of mechanical actuation system is a rack and pinion mechanism (Actuator Wikipedia, 2019).

Table 5 - Comparison between different actuators

Actuator Comparison				
	Pneumatic Actuator	Hydraulic Actuator	Electric Actuator	Shape Memory Alloy (SMA)
Advantages	Generate precise linear motion Inexpensive	Rugged and high force Can hold force and torque constant	High precision Less noise	Self-powered Accuracy
Disadvantages	Compressed air Difficulty in controlling pneumatic actuator using EMG signals	Incompressible fluid leakage Difficult to accommodate the parts for this actuator	Expensive Installation problem	Expensive

5.2 Actuator module for the hand exoskeleton

A linear servo actuator was used as the actuation mechanism for the hand exoskeleton. As seen in table 2, though pneumatic and hydraulic actuator was inexpensive to use, major drawback was the use of compressed air in case of pneumatic actuators and use of incompressible fluid for hydraulic actuator.

A linear servo actuator was used to actuate each finger exoskeleton links separately. Four actuators were used to control the range of motion one for each finger separately. A rack and pinion mechanism was used to design a linear servo actuator.

5.2.1 Rack and pinion mechanism

A rack and pinion mechanism is a type of a linear actuator. It comprises of an engaging linear gear which is known as rack and a circular gear which is known as pinion. It operates to convert rotational motion to linear motion or vice-versa. When a pinion is driven rotationally, it causes a rack to be driven linearly. And when a rack is driven linearly, it causes a pinion to be driven rotationally (Rack and Pinion Website, 2019). A rack and pinion mechanism is illustrated in the figure.

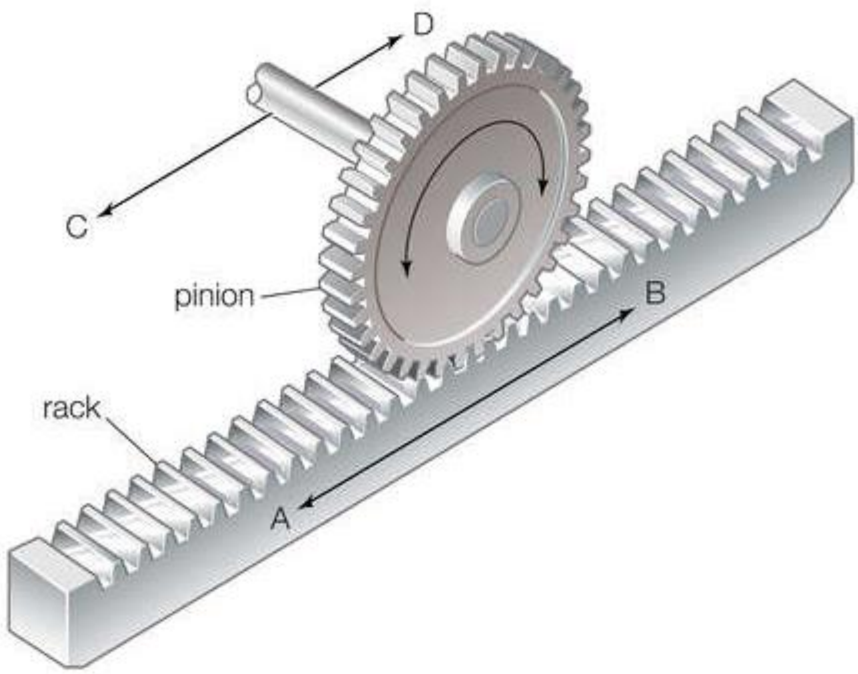

Figure 32 - Rack and pinion mechanism

In the actuator module designed for the hand exoskeleton, pinion was attached to the continuous servo motor FS90R. Servo motor was programmed using Arduino UNO board and the motors were connected to the servo driver board, PCA9685. First the servo motor connected to the pinion was driven which drove the rack linearly.

The actuator module designed for the hand exoskeleton is shown in the figure below.

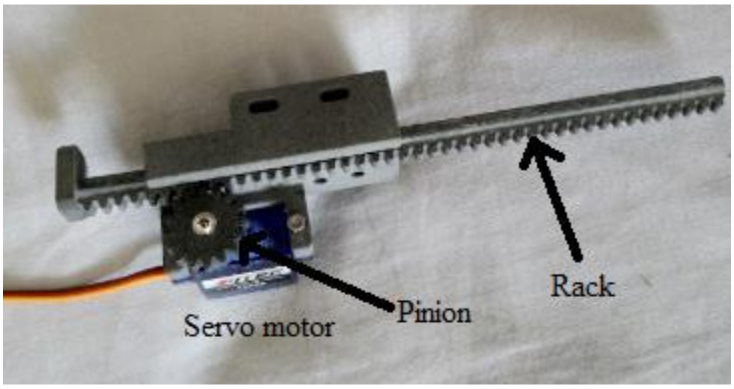

Figure 33 - Linear servo actuator designed for the hand exoskeleton

5.2.2 PCA9685 Servo Driver Module

This is an I2C bus-controlled driver board to control multiple servo motors (continuous or normal position-controlled servos). This driver board makes use of PWM (Pulse Width Modulation) pulses to control the speeds of the servo motors. It is a 16 channel 12-bit driver board, which allows to control 16 servo motors simultaneously (Adafruit website, 2012). This board can be easily interfaced with Arduino and Raspberry-pi. This driver module was used to avoid communication interference while establishing connection between Arduino board, MYO armband and the servo motors.

For this project, 4 FITEC servo motors FS90R used in the actuator module, were connected to the pca9685 module. Then the Arduino UNO board was connected to the PCA9685 module by connecting SDA, SCL, GND and VCC pins together.

The circuit connection showing the servo motors connection is shown in the figure below.

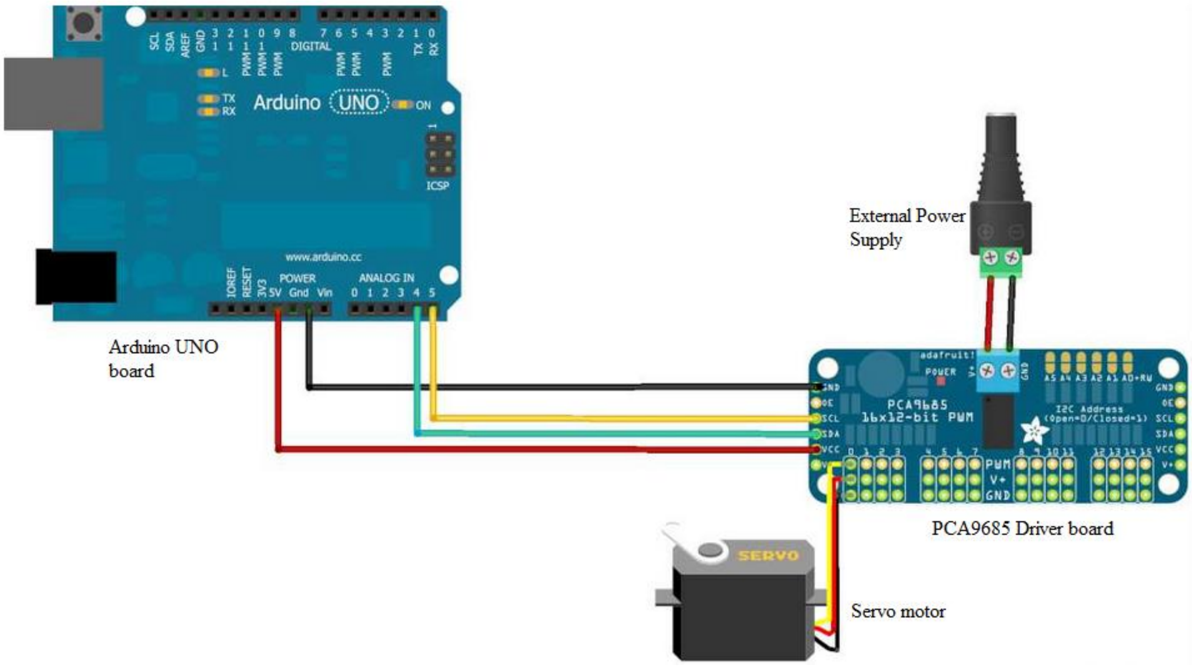

Figure 34 - Circuit connection between Arduino UNO, PCA9685 and Servo motor

As shown in the figure 34, an external 6V, 3A power supply was used to power four servo motors used in the actuator module for the exoskeleton.

6 CONTROL MECHANISM

This chapter discusses about the control mechanism used to control the trajectory of the hand exoskeleton. It also discusses about different motions of the hand controlled.

6.1 Why muscle signals?

Muscle signals, also known as Electromyogram (EMG), are generated when the muscles contract or the joints are extended or flexed. Muscles that control the movement of the fingers are in the forearm and palm. Muscles are responsible for controlling the flexion (bending), extension (straightening), adduction, abduction and circumduct as well. Muscles are divided broadly into two categories, extrinsic and intrinsic muscles. Extrinsic muscles comprise of long extensors and flexors, originate external to the hand. Whereas, intrinsic muscles originate within the hand (especially palm and wrist). Extrinsic muscles are responsible for gross movements of the hand and force gripping movements, and intrinsic movements are responsible for fine hand movements. The flexors and extensors attached to the fingers allows in bending and straightening of the fingers (Hand Wikipedia, 2019).

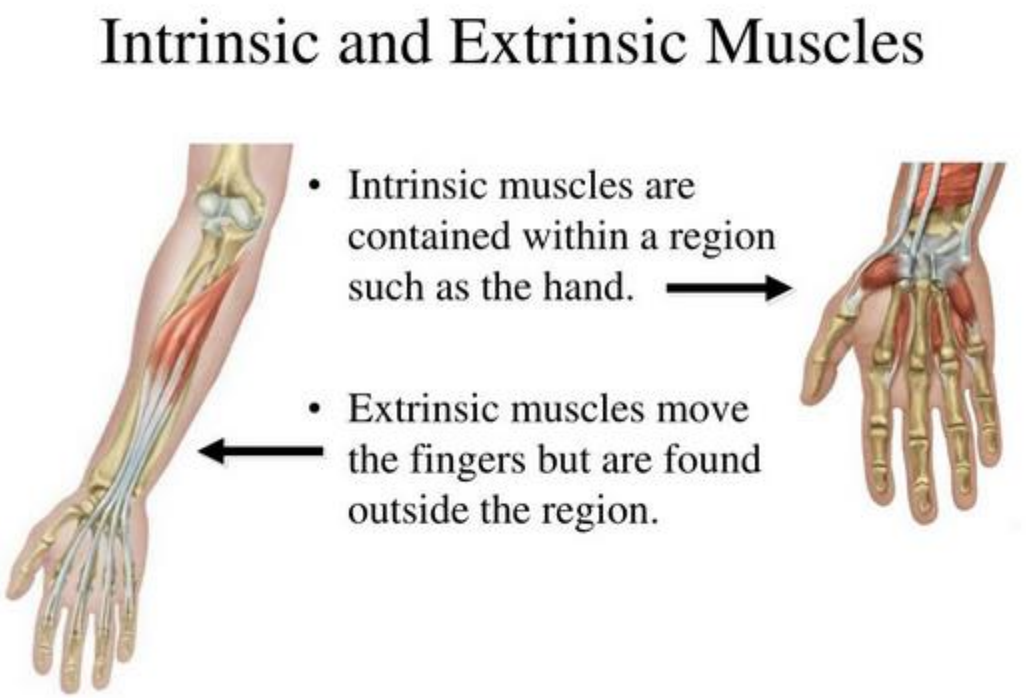

Figure 35 - Intrinsic and extrinsic muscles

Electrical activities from the muscle signals of the forearm help to know whether there is any movement in the fingers.

So, in order to improve the rehabilitation effectiveness, EMG signals were used to decide the trajectory of the hand exoskeleton.

6.2 MYO armband

To measure the electrical activity of the muscles in the forearm, there are a range of muscle sensors or EMG sensors available in the market. But MYO armband was chosen to detect the muscle signals in the forearm to control the trajectory of the exoskeleton.

MYO armband is a next generation human-machine interaction device that is used to measure the electrical activity of the muscle signals in the forearm. MYO armband is developed by the Canadian company, Thalamic Labs incorporation, which is used to measure the muscle signals produced after finger and hand movements (MYO armband website, 2013 - 2018).

MYO armband device makes use of eight medical grade stainless steel EMG sensors, a highly sensitive 9-axes IMU composed of 3-axes gyroscope, 3-axes accelerometer, 3-axes magnetometer and a vibration motor. The MYO armband is shown in the figure below:

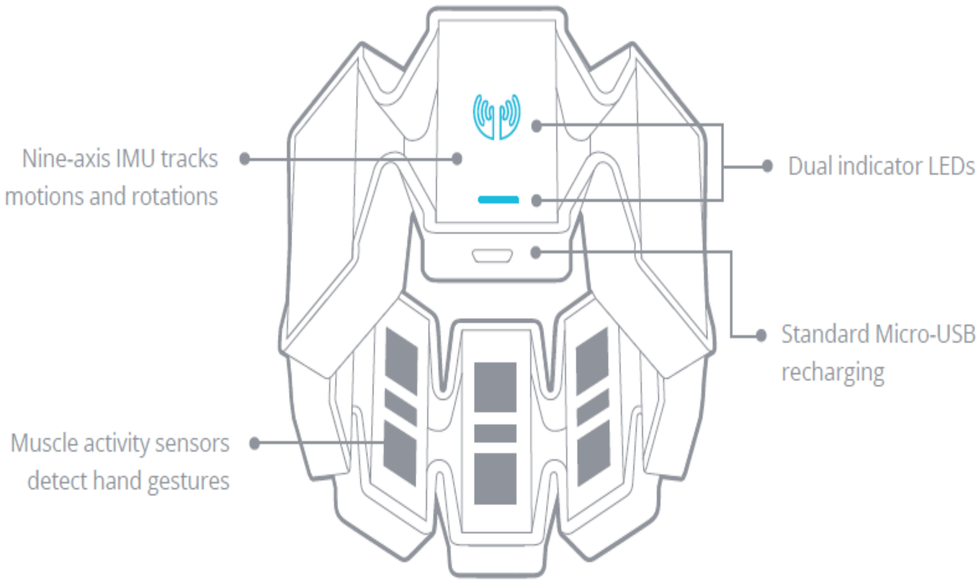

Figure 36 - MYO armband and its parts

Technical specifications of the armband are as follows:

1. Vibration motor
2. Freescale Kinetis ARM Cortex M4 120MHz MK22FN1M MCU
3. BLE NRF51822 chip
4. Inven-sense MPU-9150 at 9-axes IMU
5. 8xST 78589 operational amplifier (for each electrode)
6. 2xlithium batteries 3.7volts – 260mAh

6.3 Operation of MYO armband

MYO armband is operated by the ARM Cortex M4 processor and data transmission is controlled by the BLE NRF51822 chip. The disassembly of the MYO armband is shown in the figure.

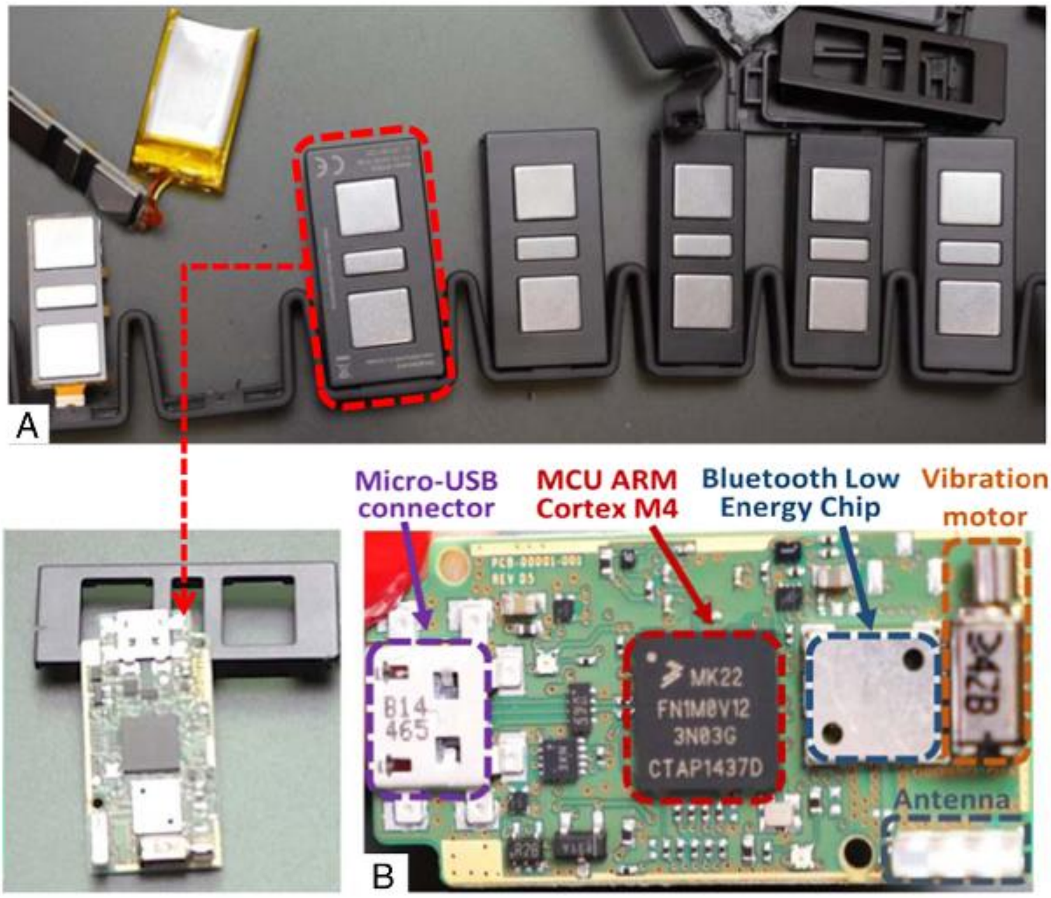

Figure 37 - Disassembly of the MYO armband

Different control modules and chips are highlighted in different colors in the figure above. As shown in the figure 37, the Micro-USB connector used for charging the armband is highlighted in purple color. The MCU ARM cortex M4 module is highlighted in red color. The Bluetooth chip, BLE NRF51822 chip, is highlighted in blue color. The vibration motor, which is used to alert the user or patient whenever an event occurs, is highlighted in brown color. In the figure 37, in grey an antenna is highlighted, which is basically used to transmit the data. Two lithium batteries, rechargeable, are indicated in figure 38.

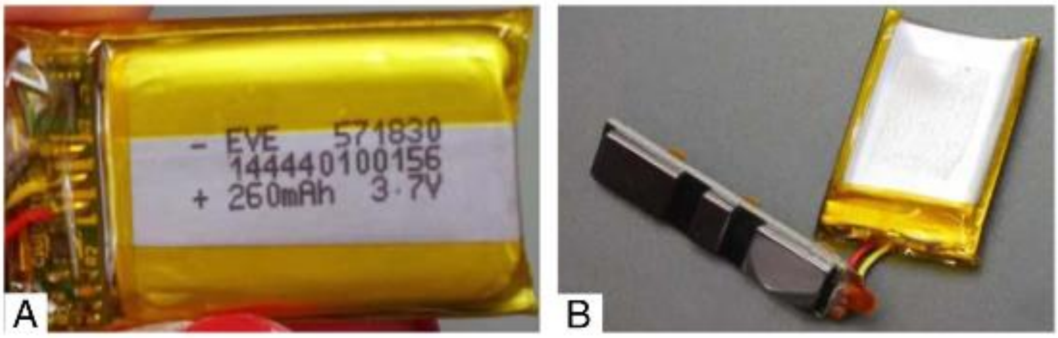

Figure 38 - Lithium batteries used in MYO armband

These batteries are recharged by 5 volts using micro-USB connector.
Figure 39 shows eight EMG surface electrodes contained in the MYO armband.

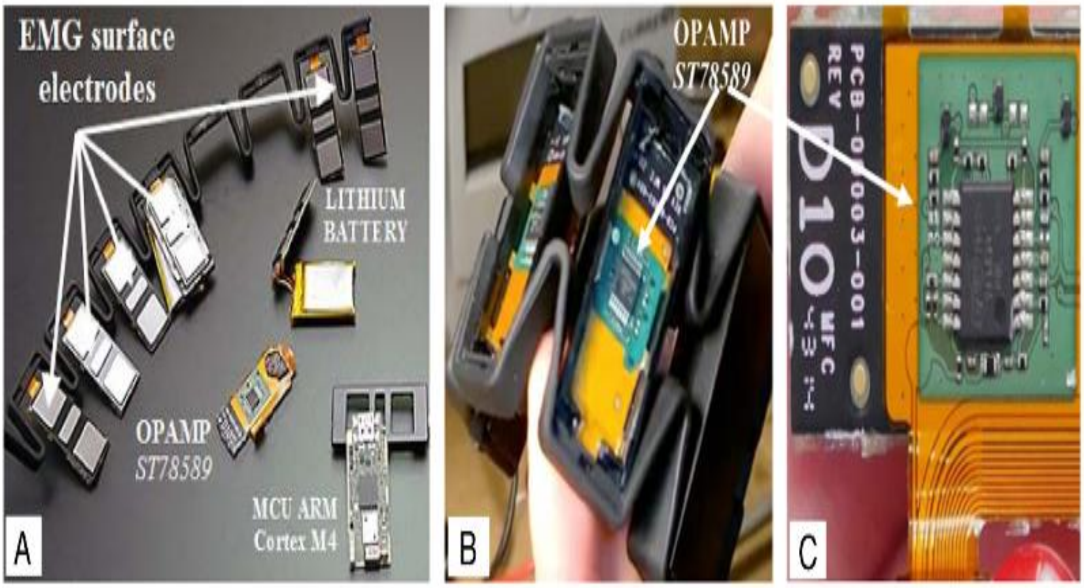

Figure 39 - EMG surface electrodes used in the MYO armband

There are different types of surface muscle electrodes in the market that are used for prosthesis or exoskeleton control. But MYO armband proves to be a better device as compared to other surface electrodes as MYO armband comes with other packed electronics. The surface electrodes can be divided into two categories: active and passive electrodes. The active electrode is comprised of three conductors, a central conductor and two conductors (One before the central conductors and the other after the central conductors). The primary operation of central conductors is to detect the electrical activity of the muscles and other two conductors are used to filter out the noise in the signals. Whereas the passive electrode consists only one conductor, which needs a conductive material to couple with the skin. As shown in the figure 39, EMG sensors are in eight different locations of the MYO armband. These EMG sensors are used to detect the electrical activity of the muscle signals in the forearm. Figure 39B and 39C shows operational amplifier ST78589, which is used to amplify the signals obtained from the EMG surface electrodes (Paolo, Federico, Giovanni, & Patrizio, 2018).

6.4 Gesture Recognition and Identification using MYO armband

MYO armband is developed by Thalamic Labs incorporation. MYO connect application is used to interface MYO device with the PC or laptop. MYO connect has a default profile stored within it. This default profile consists of five pre-defined gestures.

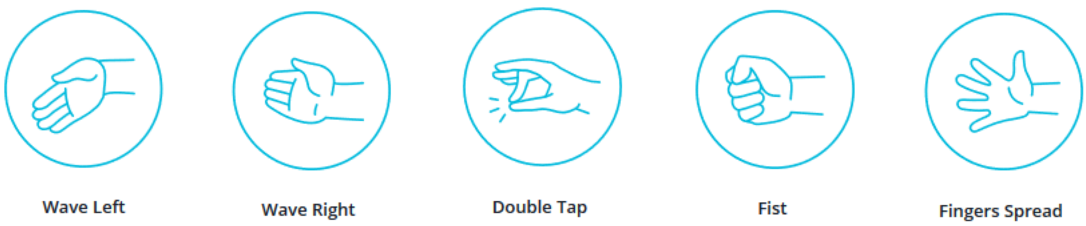

Figure 40 - Gestures detected using MYO armband

To create custom gestures, GRT's machine learning library could be used to create custom gestures. To enter the train data in order to learn a specific gesture CollectRaw executable is used. And to train the entered data to learn a specific gesture ProcessRaw executable is used. Once the data is trained for a specific gesture API's of this library can be used easily (MYO API, Devpost Website).

The gesturedevicelistener.h file of the API needs to be included which helps to extend the device listener class GestureDeviceListener.

6.5 *Exoskeleton control using MYO armband*

When a patient is recovering after stroke or accidents, there are chances that muscles controlling the finger movements might still be affected. So, the exoskeleton device was not worn on the hand recovering from stroke or accidents and the MYO armband was worn on the forearm of the healthy hand. The electrical activity from the muscle signals worn on the forearm was measured. And the data was used to control the exoskeleton device. As exoskeleton was designed for performing rehabilitation exercises, MYO armband was used to perform the closing and opening operation of the exoskeleton (Flexion and extension of the fingers).

The MYO armband was connected to the laptop using a low energy 4.0 USB Bluetooth adapter. After the connection was established, MYO connect application was used to train the armband with the muscle signals of the forearm. Once the armband was trained with the poses like flexing the finger/ fingers and extending the finger/ fingers, the armband was connected to the Arduino UNO board by using MYODuino library (Jake Chapeskie Website, 2018).

For extracting the EMG data from the armband, Visual Studio 2017 IDE was used, and coding was done in C++. The data was logged in .csv file as soon as the data was read from the MYO armband.

The following figure shows the terminal to establish the connection with the Arduino board by selecting the COM port to which the Arduino UNO board is connected.

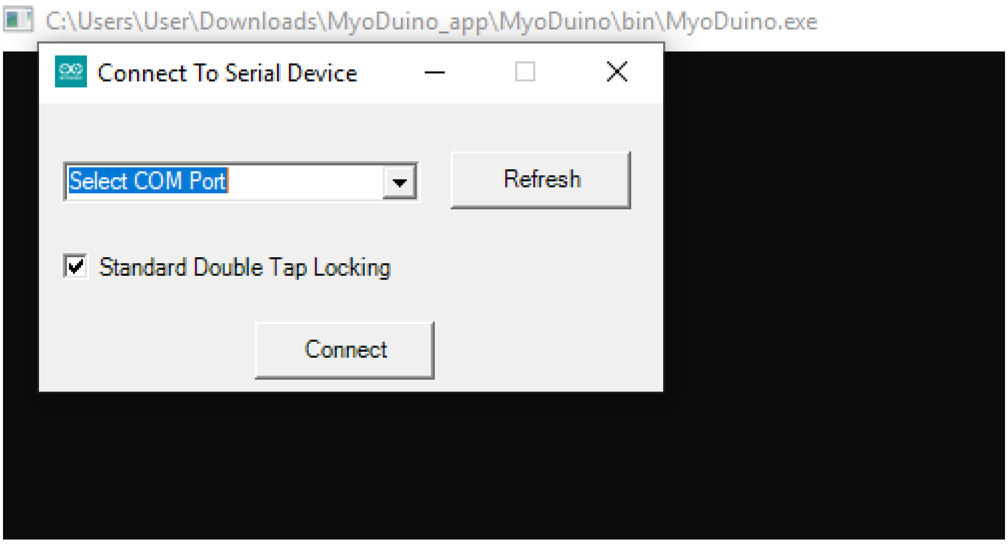

Figure 41 - Figure indicating the terminal to connect the MYO device with the Arduino board

7 3D DESIGNING AND PRINTING MATERIAL CHARACTERISTICS

In this chapter, 3d designing of the exoskeleton is discussed. Finite element analysis (FEA) of the links in the linkage structure of the finger exoskeleton is also discussed. Properties of the material used for 3d printing the exoskeleton is also discussed. Material used is also compared with the other materials available for 3d printing.

7.1 3D designing

Autodesk Fusion 360 software was used to 3d design the exoskeleton. Entire exoskeleton was designed to have small parts to be fixed together with screws. This made designing easy. As four fingers have three phalanges, the 3d design of the fingers also had three distinct parts one for each phalange. Each part was connected to the other with the help of pivot joints, which helped to fix the exoskeleton on the finger properly and allowed smooth movement. Measurements of each finger was taken to design the finger exoskeletons. These measurements are available in the Appendix section of the thesis. Link lengths were designed by taking into consideration the measurement of the fingers. Only little finger had different length links because of the size of the finger otherwise the link lengths were same for rest of the fingers. For the exoskeleton part that went on the dorsal part of the hand was designed by taking into consideration the measurements of the dorsal part of the hand and the wrist of the hand. The connectors and sliding rods on top of the base part of the exoskeleton were designed based on the measurements of the dorsal part of the hand, wrist measurements, last link of each finger.

7.2 Adaptation of the Exoskeleton design for different users

The current design of the hand exoskeleton is not adaptable to be used by different patients. But the current design can be adapted to different patients by generalising the design parameters. The basic parameters that are needed to design the finger exoskeleton are:

1. Distance between tip of the distal phalange and bottom of the proximal phalange
2. Length of all three phalanges of the finger
3. Width of the phalange

Sketch equations could be defined to take inputs in the form of length of the complete finger, length of all three phalanges of the finger and width of phalanges. After taking these inputs, operations on the sketches could be performed by using sketch equations and parameters. This would help to generate finger exoskeleton with different parameters for different patients.
This methodology has not been tried and would be used as a future work for this project.

7.3 Finite element analysis (FEA)

FEA is nothing but the simulation of given physical phenomenon by using a numerical technique (Finite element method (FEM)). This method helps to resolve the engineering defects in the 3d designed parts and optimize the design to improve structural strength of the designed parts.

7.3.1 FEA of 3d designed links

7.3.1.1 4-bar long connector

Table 6 - Stress parameters for the 4-bar long connector

Stress		
Von Mises	3.254E-07 MPa	0.8306 MPa
1st Principal	-0.128 MPa	0.5155 MPa
3rd Principal	-0.9971 MPa	0.149 MPa
Normal XX	-0.9967 MPa	0.1703 MPa
Normal YY	-0.2345 MPa	0.1838 MPa
Normal ZZ	-0.3441 MPa	0.5084 MPa
Shear XY	-0.1548 MPa	0.1421 MPa
Shear YZ	-0.06462 MPa	0.08116 MPa
Shear ZX	-0.2124 MPa	0.2625 MPa

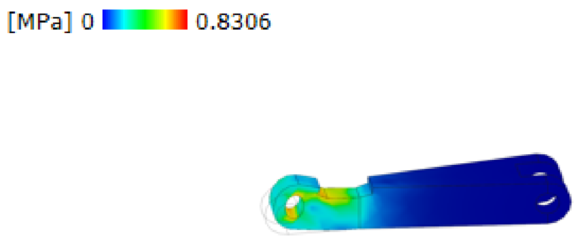

Figure 42 - Figure indicating FEA for 4-bar long connector

7.3.1.2 4-bar connector for proximal phalange

Table 7 - Stress parameters for the 4-bar connector for proximal phalange

Stress		
Von Mises	9.167E-06 MPa	0.1914 MPa
1st Principal	-0.08047 MPa	0.2342 MPa
3rd Principal	-0.2027 MPa	0.04389 MPa
Normal XX	-0.1981 MPa	0.06995 MPa
Normal YY	-0.1654 MPa	0.2108 MPa
Normal ZZ	-0.1102 MPa	0.1115 MPa
Shear XY	-0.06689 MPa	0.0671 MPa
Shear YZ	-0.0385 MPa	0.03566 MPa
Shear ZX	-0.06166 MPa	0.06164 MPa

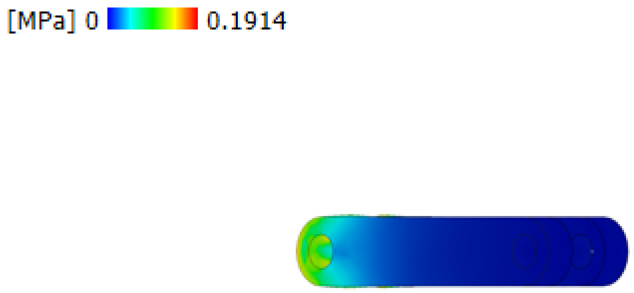

Figure 43 - Figure indicating FEA for 4-bar connector for proximal phalange

7.3.1.3 4-bar connector to connect two phalanges

Table 8 - Stress parameters for 4-bar connector to connect two phalanges

Stress		
Von Mises	6.584E-07 MPa	0.4052 MPa
1st Principal	-0.1364 MPa	0.1705 MPa
3rd Principal	-0.4491 MPa	0.02636 MPa
Normal XX	-0.4014 MPa	0.1353 MPa
Normal YY	-0.167 MPa	0.09761 MPa
Normal ZZ	-0.1836 MPa	0.08006 MPa
Shear XY	-0.08193 MPa	0.1158 MPa
Shear YZ	-0.04956 MPa	0.05121 MPa
Shear ZX	-0.05261 MPa	0.09318 MPa

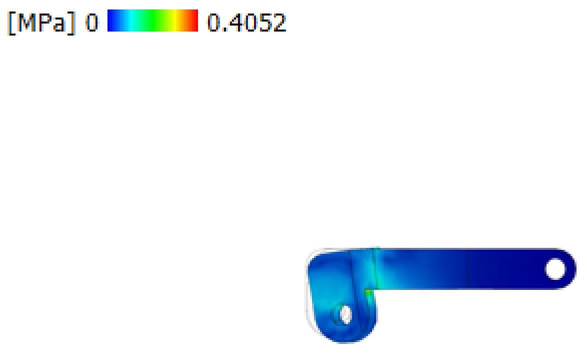

Figure 44 - Figure indicating FEA for 4-bar connector connecting two phalanges

The material used to perform the analysis of all three parts was PC-ABS plastic. Above mentioned connectors have a factor of safety (FOS) of 8 which means it can handle loads of up to 8 Newtons.

7.4 Material used

Material that was used to 3d print the exoskeleton was PC-ABS. It is the combination of the two durable thermoplastics polycarbonate (PC) and Acrylonitrile Butadiene Styrene (ABS). PC-ABS is the blend which provides heat resistance, high material strength of PC and flexibility of the ABS material (Hardie Polymers Website, 2019).

Figure 45 - PC and ABS material used in 3d printing

Initially, the exoskeleton was printed with the PLA (Polylactic Acid). But because of the low material strength, some of the parts printed with the PLA broke off easily. The index finger exoskeleton printed with the PLA material is shown in the figure below.

Figure 46 - Index finger exoskeleton printed with PLA material

7.4.1 Polycarbonate material

Polycarbonate is an amorphous, transparent, tough and a high-performance thermoplastic polymer used as a 3d printing material. The functional group of PC comprises of carbonate groups (-O-(C=O)-O-) (Omnexus Website, 2019).

Main properties of the polycarbonate material are:

1. Greater impact strength
2. Good electrical insulation
3. High shear and tensile strength
4. Low deformation under loads
5. Excellent material strength at higher temperatures

The strengths and limitations of the polycarbonate material for 3d printing is listed in the table

Table 9 - Strengths and limitations of the polycarbonate (PC) material

Strengths	Limitations
High transparency	Easily attacked by the bases and the hydrocarbons
High toughness (even at lower temperatures up to -20 degrees)	Mechanical properties degrade after temperatures greater than 60 degrees
Higher mechanical retention (up to temperature 140 degrees)	Pre-processing drying is required
Flame retardant	Low fatigue endurance
Good insulation (not affected by water or temperature)	Mechanical parts become yellowish in color after being exposed to the UV rays
Good abrasion resistance	
Withstands repeated steam sterilisations	

7.4.2 Comparison of PLA, ABS, PC and PC-ABS (Creative Mechanisms Website, 2016)

Table 10 - Comparison of PLA, ABS, PC, PC-ABS

Plastic	PLA	ABS	PC	PC-ABS

Chemical Formula	(C3H4O2)n	$(C_8H_8)x.(C_4H_6)y.(C_3H_3N)z$	$C_{15}H_{16}O_2$	
Petroleum based	Derived from sugarcane or corn starch	Yes	Yes	
Shrink rate	PLLA: 0.37-0.41% (0.0037 – 0.0041 in/in)	0.5 – 0.7 % (0.005 – 0.007 in/in)	0.6 – 0.9 % (0.006 – 0.009 in/in)	0.5 – 0.7% (0.005 – 0.007 in/in)
Thermoplastic or Thermoset	Thermoplastic	Thermoplastic	Thermoplastic	
Melting Point	PLLA: 157 - 160 ºC (315 – 338 ºF)	204 – 238 ºC (400 – 460 ºF)	288 – 316 ºC (550 – 600 ºF)	260 – 270 ºC
Mold temperature	PLLA: 178 – 240 ºC (353 – 464 ºF)	63 – 85 ºC (145 – 185 ºF)	82 – 121 ºC (180 – 250 ºF)	70 – 90 ºC

Mold Pressure		69 – 103 MPa (10,000 – 15,000 PSI)	69 – 103 MPa (10,000 – 15,000 PSI)	
Tensile Strength	PLLA: 61 – 66 MPa (8840 – 9500 PSI)	46 MPa (6,600 PSI)	59MPa (8,500 PSI)	5,800 – 9,300 PSI
Flexural Strength	PLLA: 48 – 110 MPa (6,950 – 16,000 PSI)	74 MPa (10,800 PSI)	93 MPa (13,500 PSI)	68 MPa (9,800 PSI)
Unique characteristics	Biodegradable	Readily available, cheap, durable	Extremely high impact resistance, Translucent	Extremely high impact resistance, high material strength, flexibility

8 HIGH LEVEL DESIGN OF THE SYSTEM

This chapter discusses about the high-level design of the entire system for rehabilitation of patients recovering from accidents or stroke.
High level design of the system is categorised into two broad categories:

1. Hardware design
2. Software design

8.1 *Hardware design*

Hardware components that were used for controlling the hand exoskeleton are listed as follows:

1. MYO armband
2. Arduino UNO
3. Arduino to laptop connector
4. PCA9685 servo driver board
5. 4 Continuous rotation servo motors FITEC FS90R
6. Laptop
7. Low energy 4.0 USB Bluetooth adapter
8. External 6V, 3A power supply
9. Jumper wires.

The exoskeleton was 3d designed and printed using PC-ABS material. The 3d printed exoskeleton was woven on a hand glove using Velcro straps. MYO armband device was used to control the trajectory of the exoskeleton device. Four continuous servo motors were used to design linear actuators using rack and pinion gear mechanism and the designed actuators were used to actuate the exoskeleton device. Servo motors were connected to the PCA9685 servo driver board and they were powered by the external 6V, 3A power supply. This PCA9685 board was connected to the Arduino board and the servo motors and the MYO device were controlled by the Arduino board by coding in the C++ language using Arduino IDE. Laptop was used to interface the exoskeleton device, actuator module, the MYO armband and other electronics. 4.0 low energy USB Bluetooth module was used to communicate with the MYO armband.

8.2 Software design

Block diagram indicating the design of the entire system is shown in the figure

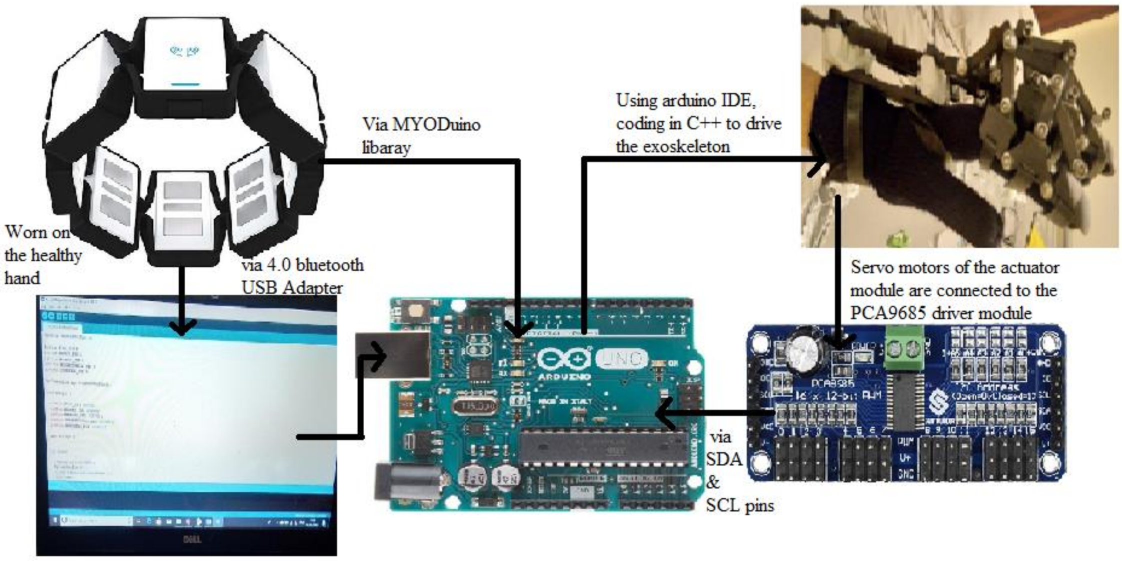

Figure 47 - Block diagram of the system

As shown in the block diagram indicated in figure 46, the communication between the Arduino board and the MYO armband was established with the help of the USB Bluetooth adapter. MYODuino software application was used to enable communication between the Arduino board and the MYO armband. Based on the pose received from the MYO armband based on the EMG signals, the actuators were actuated which eventually actuated the hand exoskeleton. Coding was done in C++ language. A separate C++ code was written to extract the EMG signals from eight EMG sensors of the MYO armband. The acceleration and angular velocity data was also extracted for the trajectory when switching from closed fist position of the hand and complete finger spread position of the hand exoskeleton.

The detailed low-level implementation of the design is discussed in the next section.

9 LOW-LEVEL IMPLEMENTATION

Low level implementation of the system can be divided into two sections as follows:

1. Hand pose detection using MYO armband
2. Controlling the trajectory of the exoskeleton

9.1 Hand pose detection using MYO armband

Hand position detection and interpretation can be divided into three main parts:

1. Signal Acquisition
2. Signal Amplification
3. Signal Analysis and interpretation

9.1.1 Signal Acquisition

Electrical activity is generated whenever the muscles are flexed or extended. There are many devices in the market that are used to detect the electrical activity of the muscle signals. Traditional sensors are comprised of electrodes, which are sticker like structures. These electrodes are attached to the skin directly, sometimes even gel is used to improve the accuracy of the signals.

The MYO armband makes use of eight EMG sensors each comprised of non-sticky electrodes. It was possible to get accurate readings regardless the type of electrodes. The detailed description of the technical features of the MYO armband is discussed in section 6 of the thesis.

9.1.2 Signal Amplification

The next step after acquiring the activity of the muscle signals is signal amplification. The amplitude of the EMG signals is generally weak when acquired from the electrodes. It is usually in the range of micro Volts (µV) and milli volts (mV) (which is usually 0-6 mV peak-to-peak or 0-1.5 mV RMS). The distribution of the EMG signals is within the range of 0 – 500 Hz frequency domain. The dominant components of the signals lie within the frequency range of 50 – 150 Hz and the signals captured outside the range of 0 – 500 Hz are usually ignored as these are the low energy signals which are not useful. There are four main types of noise that hamper the signal acquired during the process of signal acquisition. These noises are

1. Inherent noise: which is the noise of the electronic parts that form a part of muscle signal detection
2. Ambient noise: Caused by electromagnetic radiation in the environment
3. Quasi random nature of the firing rate
4. Movement of the cable connected to the electrode

In MYO armband, OPAMP (operational amplifier) ST78589 is used for amplification purpose. This amplifier is contained in each element of the armband. The detailed description of its technical features is discussed in section 6 of the thesis.

9.1.3 Signal analysis and interpretation

MYO connect application by the Thalamic labs is used to learn the poses of the hand based on the electrical activity of the muscle signals. It is basically a machine learning algorithm which uses the activation signal as a training data to learn the poses and improve the accuracy of the gesture. When pairing the MYO device with the laptop or PC, it needs to be worn on part on the forearm right below the elbow. Based on the electrical activity detected, it detects whether the arm is left or right, which is saved. After this armband is trained for different poses of the hand based on the detected electrical activity generated from the muscle signals (when flexed or extended to form a fist or other hand gestures). Once these hand poses are learned, every time the armband is connected to the laptop or PC and the device is worn on the forearm. As soon as the armband is worn on the forearm, it asks to sync with the connected laptop or PC by performing a hand pose. Once the device is synchronized, it can be used to control applications or other robotic devices like prosthesis or exoskeletons.
Flowchart indicating this process is shown in the figure below.

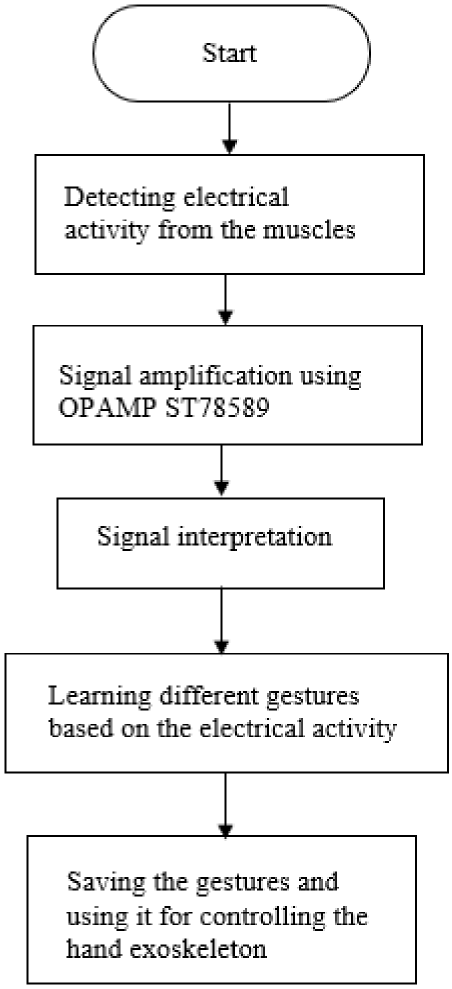

Figure 48 - Flowchart indicating hand pose detection using MYO armband

9.2 Controlling the trajectory of the exoskeleton

As the hand exoskeleton was designed for performing rehabilitation exercises by the patients recovering from accident or stroke, open and closed position of the hand was targeted to decide the trajectory of the exoskeleton.

The system was designed to have three defined states: rest, open and closed. As a robot is always in a defined state, finite state machine (FSM) was used to design the system.

Schematic of the FSM for the system is shown in the figure 48.

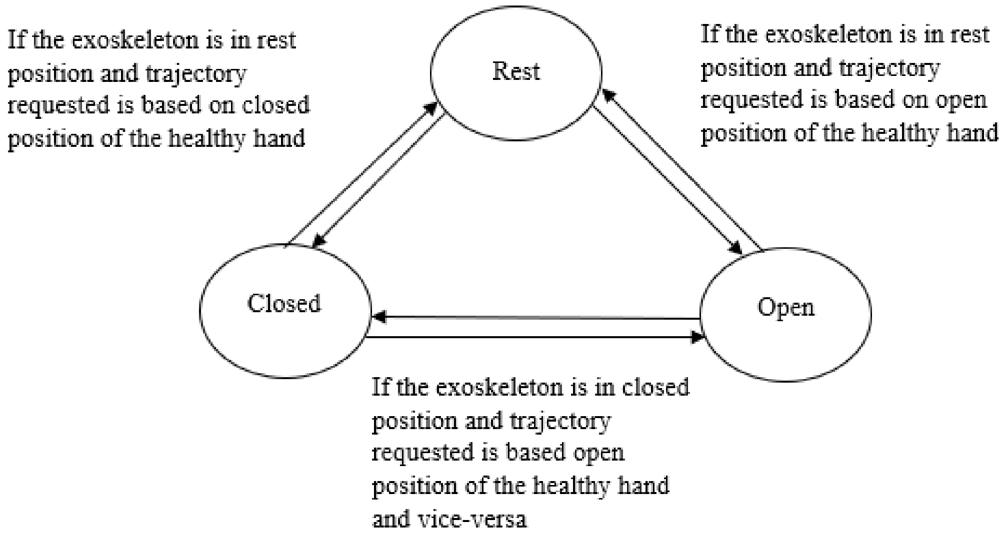

Figure 49 - Schematic of the FSM for the system

In rest state, the servo motors connected to the finger exoskeleton were reset. Trajectory of the exoskeleton was decided based on the electrical activity of the muscle signals of the healthy hand (MYO armband must be worn on the healthy hand of the patient). Flags were set when open/close trajectory for the exoskeleton was decided to enable correct performance of the exoskeleton.

The flowchart for the same is shown in the figure below

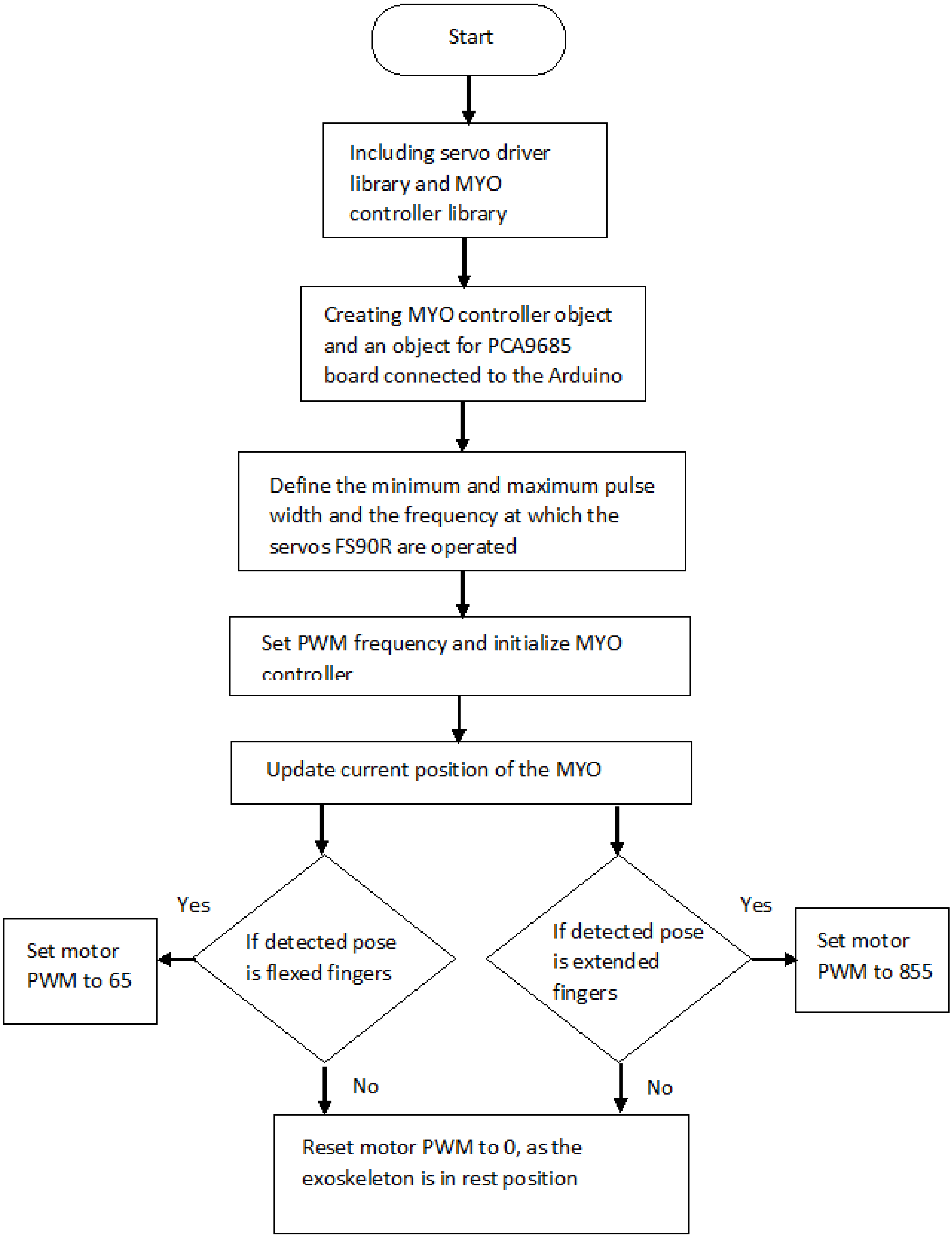

Figure 50 - Flowchart indicating trajectory decision using MYO armband

As shown in the flowchart indicated in the figure 49, the servo motors were moved by setting the PWM of continuous servo motors to different pulse width values.

The table below shows different speeds of continuous servo motor and what it indicates

Table 11 - Different speeds of continuous servo motor

Movement direction	Servo motor speed	Corresponding PWM	Fast or slow
Forward	0	85	Fast
Forward	60	65	Slow
Backward	180	965	Fast
Backward	120	855	Slow
Stop	90	0	NA

10 RESULTS AND DISCUSSION

10.1 Results

Test results captured while setting up the MYO armband device, establishing connection between MYO armband and Arduino UNO board are discussed. Acceleration and angular velocity graphs captured for open-to-close trajectory and vice versa are also discussed. Range of motion (ROM) of the hand exoskeleton device was analysed by tracker video analysis software and the results are presented and compared with the range of motion of the normal healthy hand. The system was tested by wearing the armband on both the hands.

Test results obtained while establishing connection between MYO armband and Arduino UNO board are as follows:

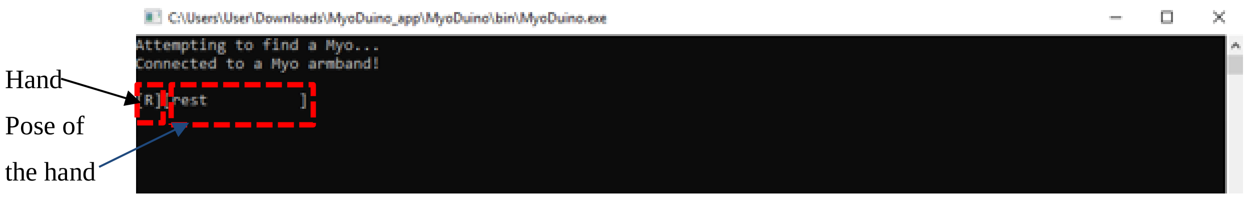

Figure 51 - Test result indicating MYO connection with Arduino (rest position)

As seen in the figure, the information whether MYO armband is connected to the Arduino or not is printed in the console. The symbol [R] indicates that the armband is worn on the right hand and [rest] indicates that the hand is in rest position.

Though only three positions were used for controlling the trajectory of the exoskeleton (rest, open and closed), two other positions of the hand were also learned: wave in and wave out.

Figures indicates other detected poses based on the electrical activity of muscle signals of the right forearm.

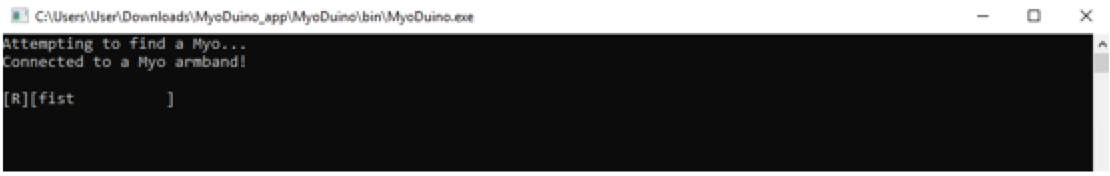

Figure 52 - Test result indicating MYO on the right hand connected with Arduino (hand closed position)

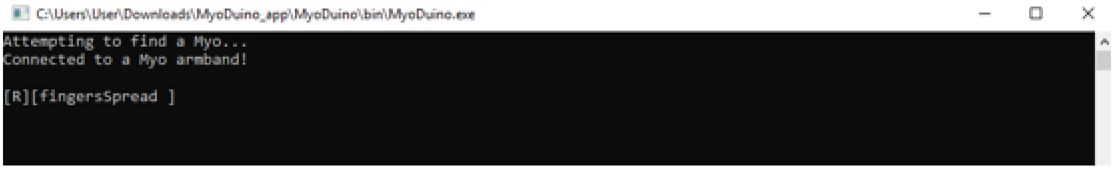

Figure 53 - Test result indicating MYO on the right hand connected with Arduino (finger stretched out)

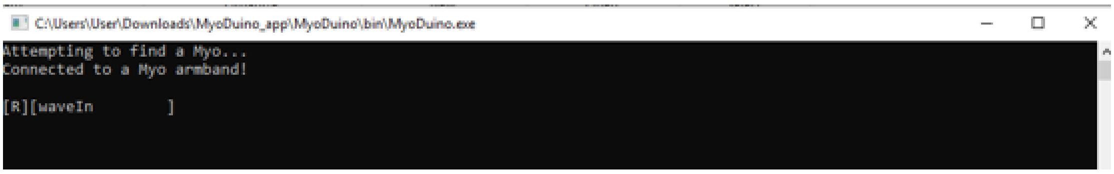

Figure 54 - Test result indicating MYO on the right hand connected with Arduino (hand waved in)

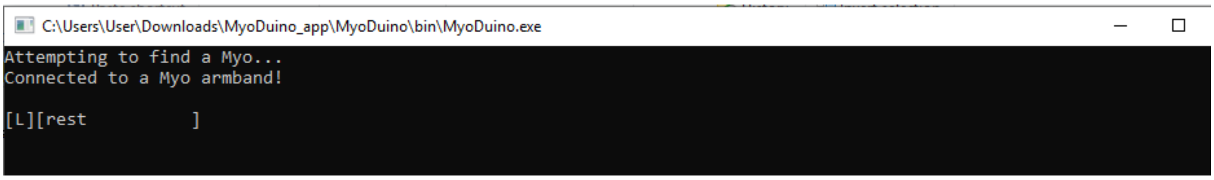

Figure 55 - Test result indicating MYO on the left hand connected with Arduino (rest position)

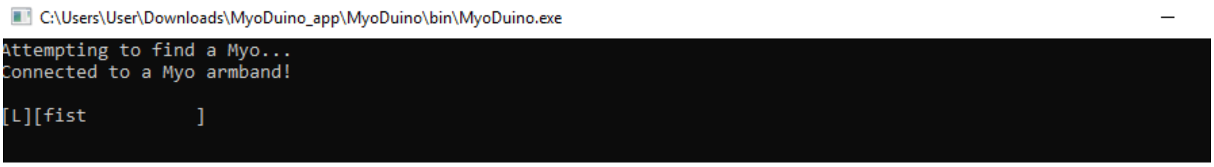

Figure 56 - Test result indicating MYO on the left hand connected with Arduino (hand closed position)

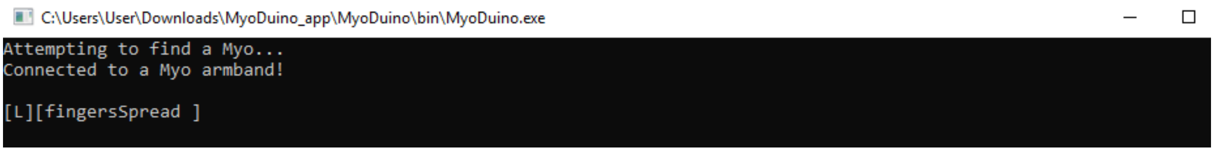

Figure 57 - Test result indicating MYO on the left hand connected with Arduino (fingers stretched out position)

Graphs indicating electrical activity of muscle signals when hand is flexed or extended to form postures like opening a hand, closing a hand, waving in, waving out, and when the hand is in rest position.

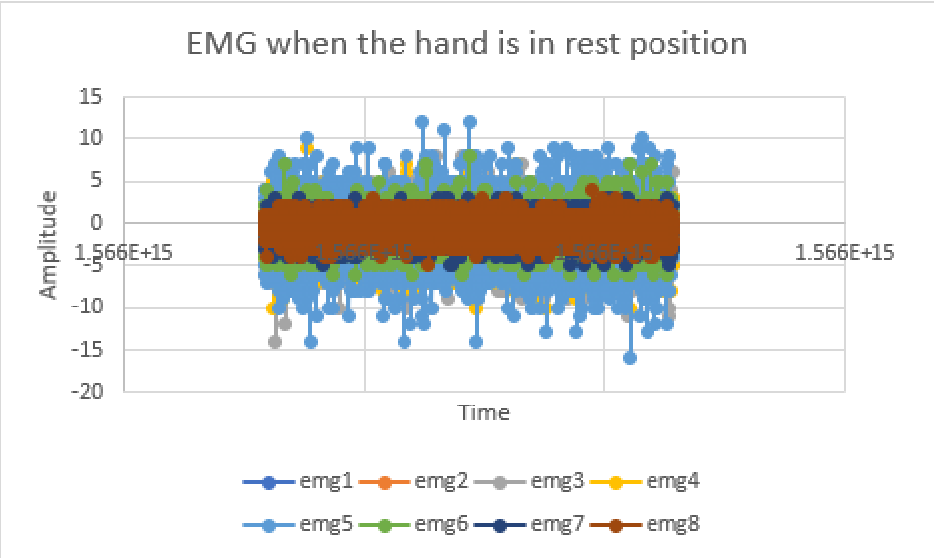

Figure 58 - Graph indicating EMG when the hand is in rest position

As shown in the figure 48, graph indicates the data captured by eight EMG sensors. The data was captured in rest position. It is evident from the figure that amplitude of the signals remains constant, which indicates that the data was captured with the hand in rest position. The data from EMG electrodes was captured at 200 Hz.

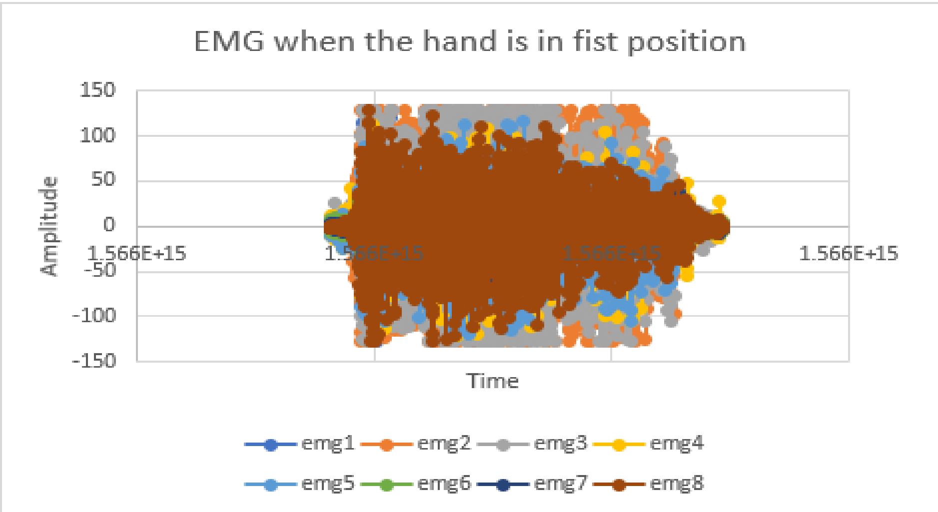

Figure 59 - Graph indicating EMG when the hand is in fist position

As shown in the figure 49, graph indicates EMG captured when the hand is in fist position. As shown in the figure, the amplitude of the signal ranges between 50 to 140 (peak-to-peak).

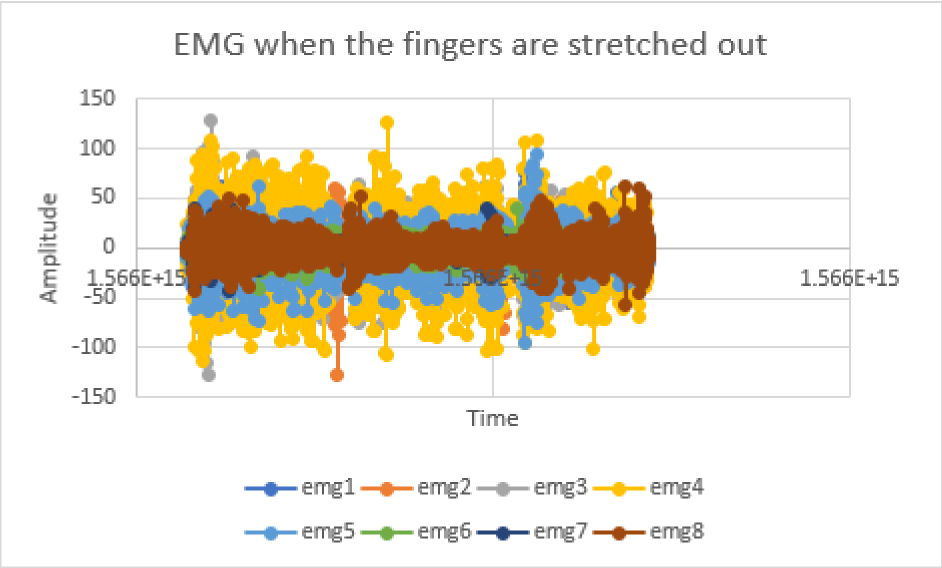

Figure 60 - Graph indicating EMG when the fingers are stretched out

Figure 50 indicates the EMG when the fingers are stretched out. Only few signals are spiked as shown in the figure. The signal amplitude ranges between 40 to 100 (peak-to-peak).

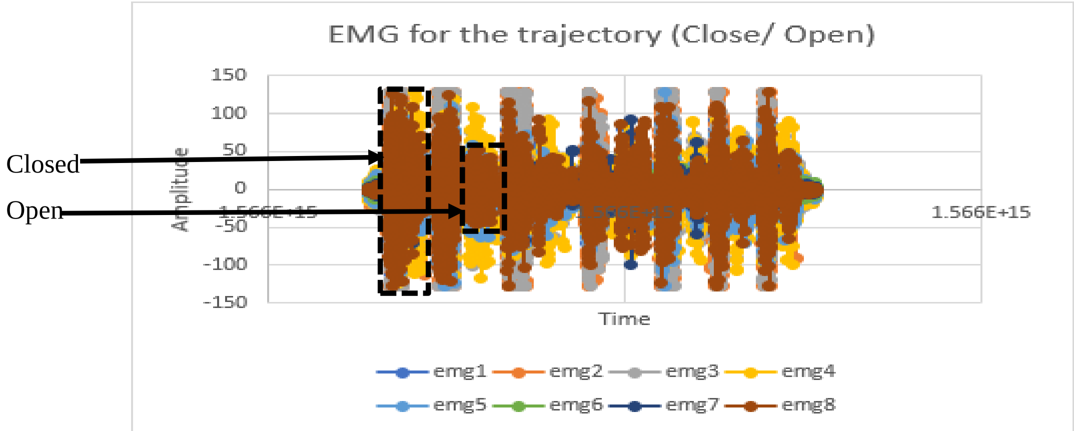

Figure 61 - Graph indicating EMG for the trajectory (Close/ Open)

Graph indicating EMG for the close – open trajectory is shown in the figure 51. It can be seen from the figure that EMG for close and open position of the hand are alternating. The signals with the amplitude 140 (peak-to-peak) indicate the closed position (fist position of the hand) and the signals with the amplitude 40 (peak-to-peak) indicate the open position (stretched out position of the fingers).

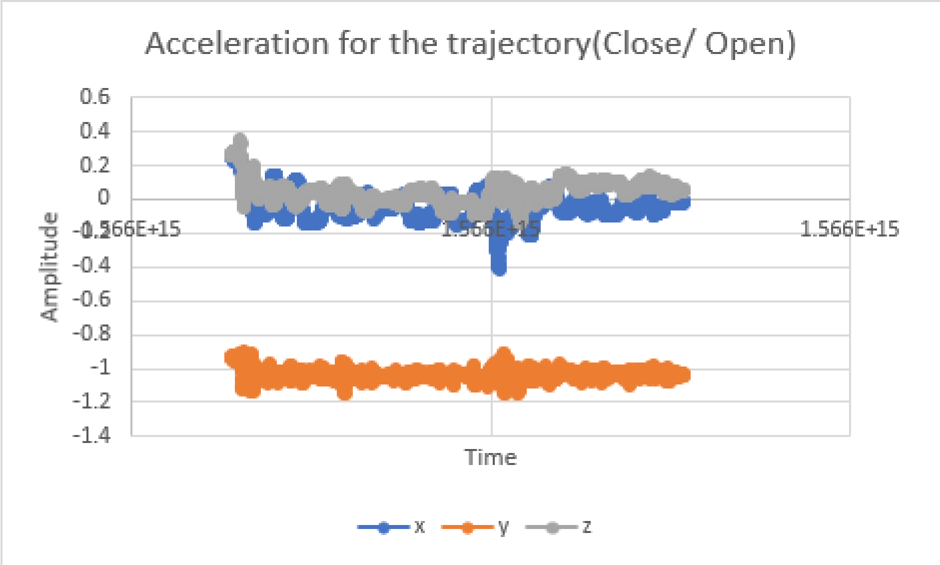

Figure 62 - Graph indicating acceleration for the trajectory (Close/ Open)

As shown in the figure 52, acceleration graph for the close – open trajectory of the hand is shown. The data is captured at 50 Hz from the 9-axes IMU contained in the MYO armband when the hand performs close – open trajectory.

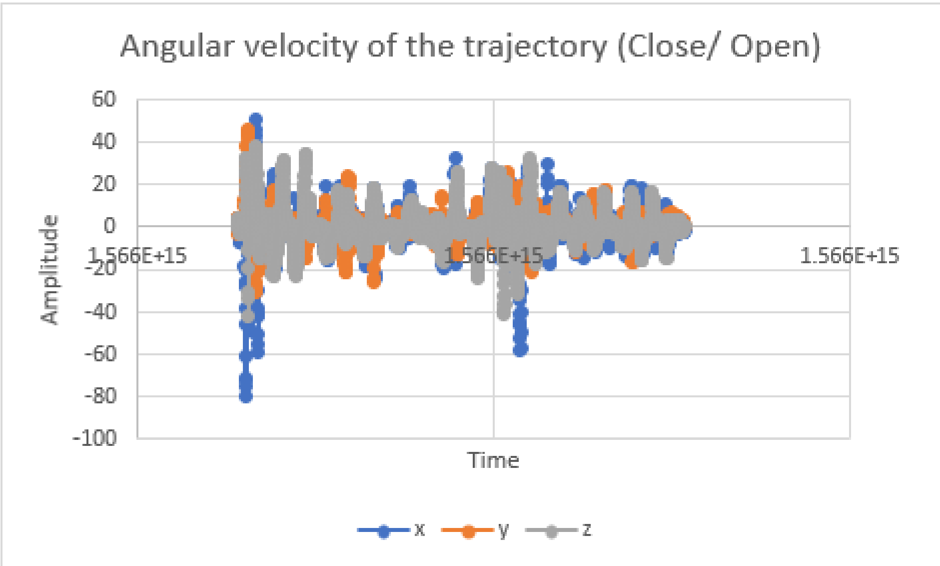

Figure 63 - Graph indicating angular velocity of the trajectory (Close/ Open)

Angular velocity of the close – open trajectory performed by the hand is shown in the figure 53. This data is also captured at 50 Hz from the 9-axes IMU contained in the MYO armband.

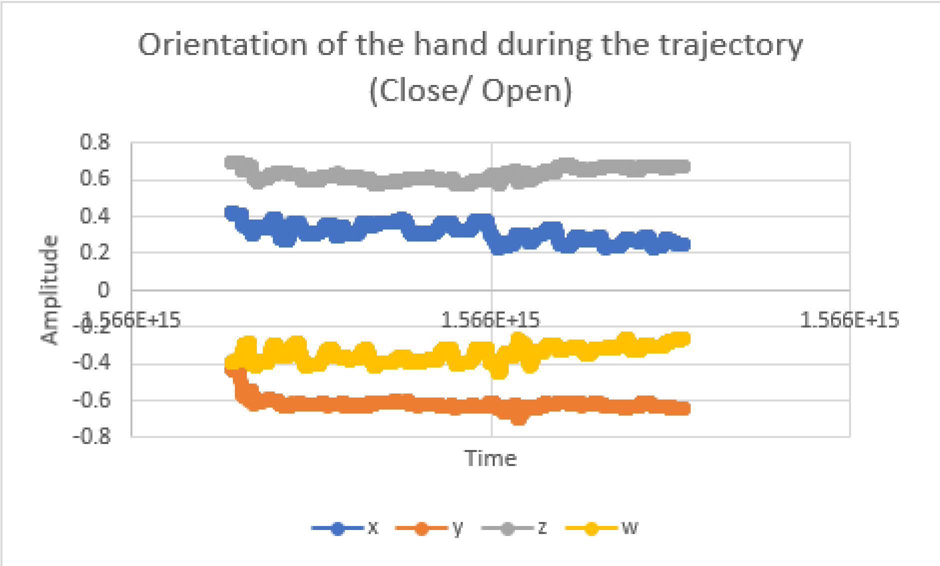

Figure 64 - Graph indicating orientation of the hand during trajectory (Close/ Open)

The graph in figure 54 indicates the orientation of the hand when performing the close – open trajectory is shown. This orientation of the hand is in 3d space and is indicated with respect to x, y, z axis.

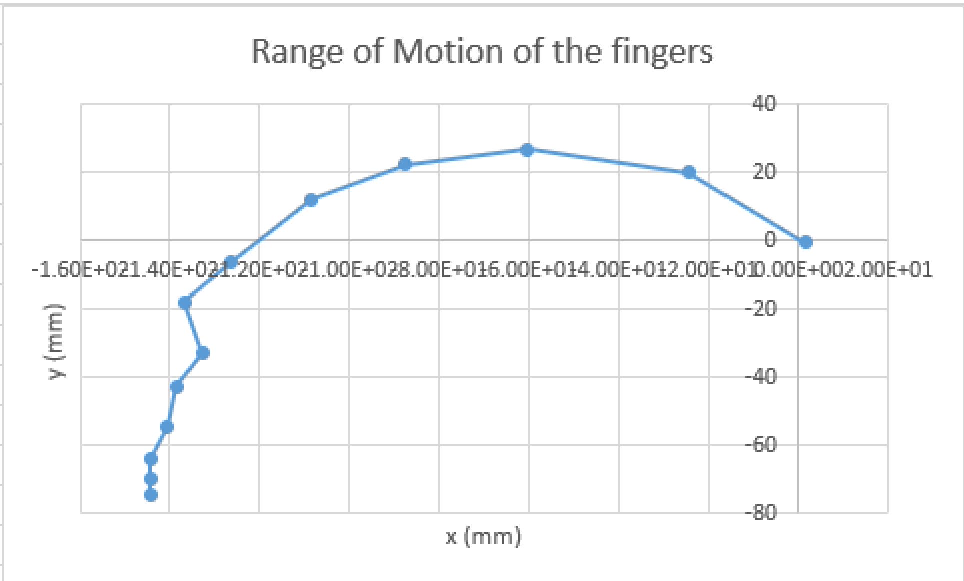

Figure 65 - Graph indicating range of motion of the fingers

Figure 55 indicates the range of motion of the fingers when using the exoskeleton for performing the rehabilitation exercises. The ideal range of motion of the finger is 110º. The range of motion obtained by using the exoskeleton was decent but less than 110º. This range of motion was obtained by designing the link lengths with the parameters as listed in the table 2.

10.2 Discussion

Figures from 50 to 56 showed that the connection was successfully established between the MYO armband and the Arduino UNO board. Testing was carried out by wearing the MYO armband device on both the hands. It was able to learn the pose using MYO armband from the electrical activity signals from both the hands. Figures from 57 to 60 indicates the electrical activity of the muscle signals when the MYO was worn on the forearm. Figure shown in 57 shows that the hand and fingers are in the rest position. From the graph in figure 57, the amplitude of the EMG signals remained almost constant which indicated that the fingers are in the rest position. The graph in figure 58 showed that the fingers flexed, and the amplitude of the signals was approximately 50 to 140 (peak-to-peak). The graph in the figure 59 indicated that the fingers were extended, and the muscle signals had an amplitude of approximately 40 to 100 (peak-to-peak). The graph in the figure 60 indicates the EMG graph for the close-open trajectory. The closed-open action was performed for a quite few times in a series to study the nature of the muscle signals. The signals had an amplitude of 140 (peak-to-peak) for closed position and 40 (peak-to-peak) for open position.

It was observed that the 1 DOF exoskeleton design was proper for the finger exoskeleton for four fingers of the hand. With the designed exoskeleton, the opening and closing of the hand was performed smoothly. With the design of the exoskeleton, the closing and opening of the hand was possible even without the actuator. The actuator was used to exert the force to the fingers to enable the movement of the affected fingers. The exoskeleton was designed to perform rehabilitation exercise with and without using the EMG signals. When EMG signals were used to decide the trajectory, satisfactory results were obtained. Different poses were learned, and their EMG data was captured at 200 Hz. These poses were used to control the actuators connected to the exoskeleton. The connection between the Arduino UNO, PCA9685, MYO armband and the actuator was established successfully. For actuator design, pneumatic actuators were also used. But there were difficulties in establishing communication between the pneumatic actuator, microcontroller and MYO armband, so the linear actuator was designed using the FITEC continuous servo motors by using rack and pinion mechanism.

With respect to the design of the exoskeleton, the current design provides the decent range of motion. Though with the device it is not possible to form a complete closed position of the hand (completely flexing all the fingers), the reachable space of the finger exoskeleton can be improved by adding more five-bar linkages in series with the designed linkage mechanisms.

Also, the range of motion of the finger could be further improved by increasing the lengths of the links used in the four-bar and five-bar linkages.

11 CONCLUSION AND FUTURE WORK

This chapter gives conclusions on the design and implementation of the exoskeleton for performing rehabilitation exercises when patient is recovering from the accident injury and stroke.

11.1 CONCLUSION

Thus, the exoskeleton device with 1 DOF was 3d designed successfully. The linkages designed to transmit the power to the phalanges of the finger were also designed successfully. The connection between the MYO armband, Arduino, PCA9685 and the laptop was established successfully. The results obtained by testing the system were satisfactory but there are still scopes for the improvement with respect to the design of the exoskeleton. The mechanical design of the exoskeleton was discussed successfully. The kinematic analysis of the kinematic model of the linkage structure for the exoskeleton was also discussed successfully. Different actuation mechanisms were compared, and the actuator module used for the actuating the exoskeleton was also discussed and the reason for using the designed actuator module was also discussed. The control mechanism using MYO armband was also discussed successfully. The technical features of the electronics contained within the MYO armband was also discussed. The high-level design and low-level implementation of the system was also discussed successfully. The flowcharts and state chart indicating the states of the exoskeleton was also explained. The results obtained after testing the system was also discussed.

11.2 FUTURE WORK

Future work would focus on improving the reachable space of the finger exoskeletons and 3d designing the exoskeleton for the thumb. Future work would also aim at adapting the current 3d design of the exoskeleton for multiple users. The thumb has a complex structure unlike the fingers of the hand. The thumb comprises of five DOFs, 1 DOF each at IP and MP joint of the thumb and 3 DOFs at the trapeziometacarpal joint of the thumb. There are quite few models designed for the thumb and the ones that are designed are designed to address three to four degrees of freedom. Thus, future work would aim at 3d designing the exoskeleton structure for the thumb as well. The four-bar and five-bar linkage mechanism could be used for 3d designing the thumb exoskeleton to address all the 5 DOFs. The future work would also aim at improving the resultant range of motion while flexing the fingers together by increasing the link lengths and adding more links in series with the designed four-bar and five-bar linkages.

REFERENCES

O'dell, M., Lin, C.-C., & Harrison, V. (2009). Stroke Rehabilitation: Strategies to Enhance Motor Recovery. *Annual Review of Medicine, 60*(1), 55-68.

Portnova, A., Mukherjee, G., Peters, K., Yamane, A. and Steele, K. (2018) 'Design of a 3d printed, open-source wrist-driven orthosis for individuals with spinal cord injury' in: *Public Library of Science, 13*(2).

Park, S., Weber, L., Bishop, L., Stein, J. and Ciocarlie, M. (2018) 'Design and development of effective transmission mechanisms on a Tendon Driven Hand Orthosis for Stroke Patients' in: *IEEE International Conference on Robotics and Automation.*

Lambercy, et al. (2017) 'Robotic Hand Orthosis for Therapy and Assistance in Activities of Daily Living' in: *ETH Zurich, Institute of Robotics and Intelligent Systems.*

Yamaura, H., Matsushita, K., Kato, R. and Yokoi, H. (2009) 'Development of Hand Rehabilitation System for Paralysis Patient: Universal design using wire-driven mechanism' in: *31st Annual International Conference of the IEEE EMBS*, ISBN 978-1-4244-3296-7.

Nakagawara, S., Kajimoto, H., Kawakami, N. and Tachi, S. (2005) 'An Encounter-Type Multi-Fingered Master Hand using Circuitous Joints' in: *Proceedings of the IEEE International Conference on Robotics and Automation*, ISBN 0-7803-8914-X.

Noritsugu, T., Yamamoto, H., Sasaki, D. and Takaiwa, M. (2004) 'Wearable Power Assist Device for Hand Grasping using Pneumatic Artificial Rubber Muscle' in: *13th IEEE International Workshop on Robot and Human Interactive Communication*, ISBN 0-7803-8570-5.

Wege, A. and Hommel, G. (2005) 'Development and Control of a Hand Exoskeleton for Rehabilitation of Hand Injuries' in: *Proceedings of the IEEE/RSJ International Conference on Intelligent Robots and Systems*, ISBN 0-7803-8912-3.

Ertas, I., Hocaoglu, E., Barkana, D. and Patoglu, V. (2009) 'Finger Exoskeleton for Treatment of Tendon Injuries' in: *Proceedings of the IEEE 11th Conference on Rehabilitation Robotics ICORR*: 194-201.

Di Cicco, M., Lucas, L. and Matsuoka, Y. (2004) 'Comparison of Control Strategies for an EMG Controlled Orthotic Exoskeleton for the Hand' in: *Proceedings of the IEEE International Conference on Robotics and Automation*: 1622-1627.

Jo, I. and Bae, J. (2017) 'Design and control of a wearable and force-controllable hand exoskeleton system' in: *Mechatronics Journal,* 90-101.

Bai, S. and Angeles, J. (2008) 'A unified input-output analysis of four-bar linkages' in: *Mechanism and Machine Theory*, 43(2): 240-251.

Hassaan, A., G. (2015) ‘Synthesis of Planar Mechanisms, Part VIII: Five Bar Mechanism’ in: *International Journal of Recent Engineering Science*, 17.

Paolo, V., Federico, G., Giovanni, A., Z. and Patrizio, P. (2018) ‘Technical Features and Functionalities of MYO Armband: An Overview on Related Literature and Advanced Applications of Myoelectric Armbands Mainly Focused on Arm Prostheses’ in: *International Journal on Smart Sensing and Intelligent Systems*, 11(2): 1-25.

Thomasnet Website (2016) http://www.thomasnet.com/articles/pumps-valves-accessories/types-of-actuators/ (Accessed multiple times during June-August 2019)

Machine design Website (2016) http://www.machinedesign.com/ (Accessed multiple times during July-August 2019)

Tech faq Website (2018) http://www.tech-faq.com/ (Accessed during May 2019)

Stroke Association Website (2019) http://www.stroke.org.uk/ (Accessed multiple times during July-August 2019)

MYO Armband Website (2013-2018) http://www.myo.com/ (Accessed multiple times during January 2018-August 2019).

Trombly, A.C. (1989) ‘Occupational Therapy for Functional Dysfunction’ *Lippincott Williams and Wilkins*.

Healthpages Website (2018) http://www.healthpages.org/anatomy-function/anatomy-hand-wrist/ (Accessed multiple times during May-August 2019).

Kinematics Wikipedia Website (2019) http://www.wikipedia.org/wiki/Kinematics/ (Accessed multiple times during Feb-August 2019).

Actuator Wikipedia Website (2019) http://www.wikipedia.org/wiki/Actuator/ (Accessed multiple times during June-August 2019).

Rack and Pinion Wikipedia Website (2019) http://www.wikipedia.org/wiki/Rack_and_pinion/ (Accessed multiple times during July-August 2019).

Adafruit Website (2012) http://learn.adafruit.com/16-channel-pwm-servo-driver/ (Accessed multiple times in August 2019).

Hand Wikipedia (2019) http://www.wikipedia.org/wiki/Hand/ (Accessed multiple times during May-August 2019).

Jake Chapeskie Website (2018) http://www.jakechapeskie.com/wp_dir/projects/myoduino/ (Accessed multiple times during June-August 2018).

Hardie Polymers Website (2019) http://www.hardiepolymers.com/polymers/pcabs-plastic-supplier-uk/ (Accessed multiple times during June-August 2019).

Omnexus Website (2019) http://www.omnexus.specialchem.com/selection-guide/polycarbonate-pc-plastic/ (Accessed multiple times in August 2019).

Creative Mechanisms Website (2016) http://www.creativemechanisms.com/plastics-for-prototype-parts/ (Accessed multiple times in August 2019).

After Trauma Website (2014) https://www.aftertrauma.org/life-after-trauma/rehabilitation-and-after-care (Accessed multiple times in September 2019).

National Institute of Neurological Disorders and Stroke (2019) https://www.ninds.nih.gov/Disorders/Patient-Caregiver-Education/Fact-Sheets/Post-Stroke-Rehabilitation-Fact-Sheet (Accessed multiple times in September 2019).

Saebo Website (2017) https://www.saebo.com/stroke-rehab-exercises-passive-vs-active/ (Accessed multiple times in September 2019).

Drugs.com Website (2019) https://www.drugs.com/cg/passive-range-of-motion-exercises.html (Accessed multiple times in September 2019).

Merek Manual: Physical Therapy Website (2017) https://www.msdmanuals.com/en-gb/home/fundamentals/rehabilitation/physical-therapy-pt (Accessed multiple times in September 2019).

APPENDIX

Hand and sliding rod measurements

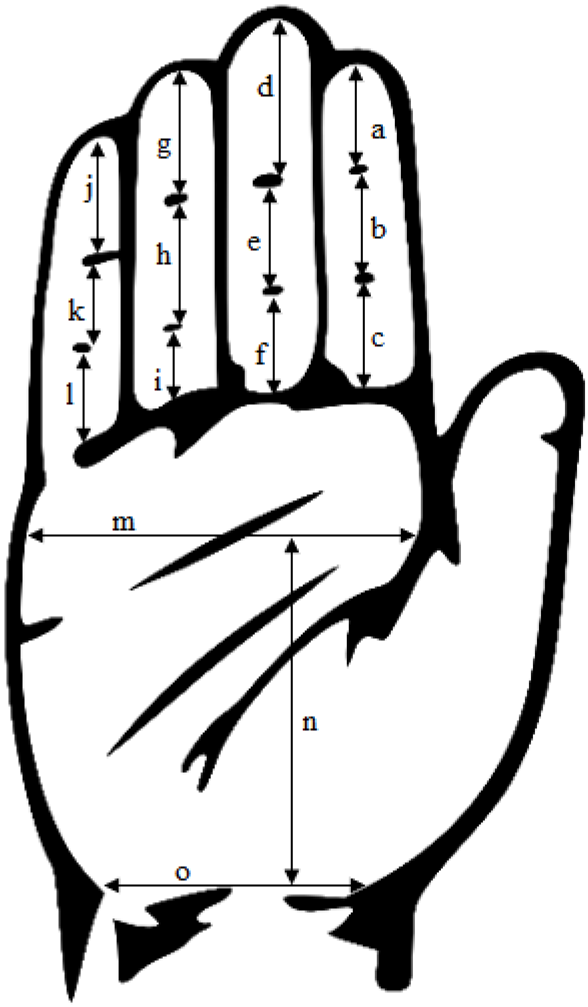

Figure 66 - Hand and finger measurements

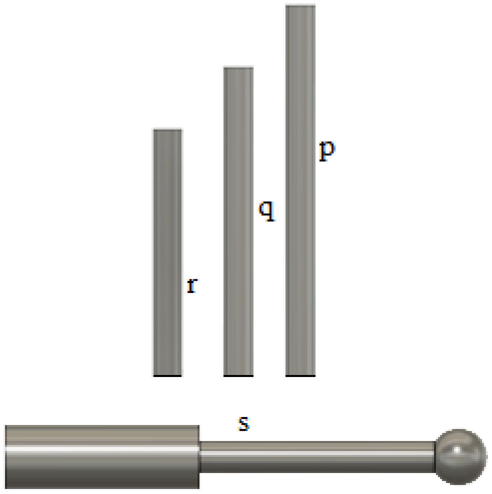

Figure 67 - Sliding rod measurements

The measurements of the hand, finger and sliding rods used for designing are mentioned in the table below:

Table 12 - Hand, finger and sliding rod measurements

Hand constants	Measurements (mm)
a	20.16
b	20.51
c	27.52
d	20.30
e	25.96
f	24.17
g	19.42
h	23.49
i	19.69
j	18.40
k	14.30
l	16.7

m	70.40
n	78.50
o	54
p	60
q	50
r	40
s	74.285

The link lengths and joint angles are already discussed in section 4, and the link lengths and the joint angles are mentioned in table 2 and 3.

Actuator measurements

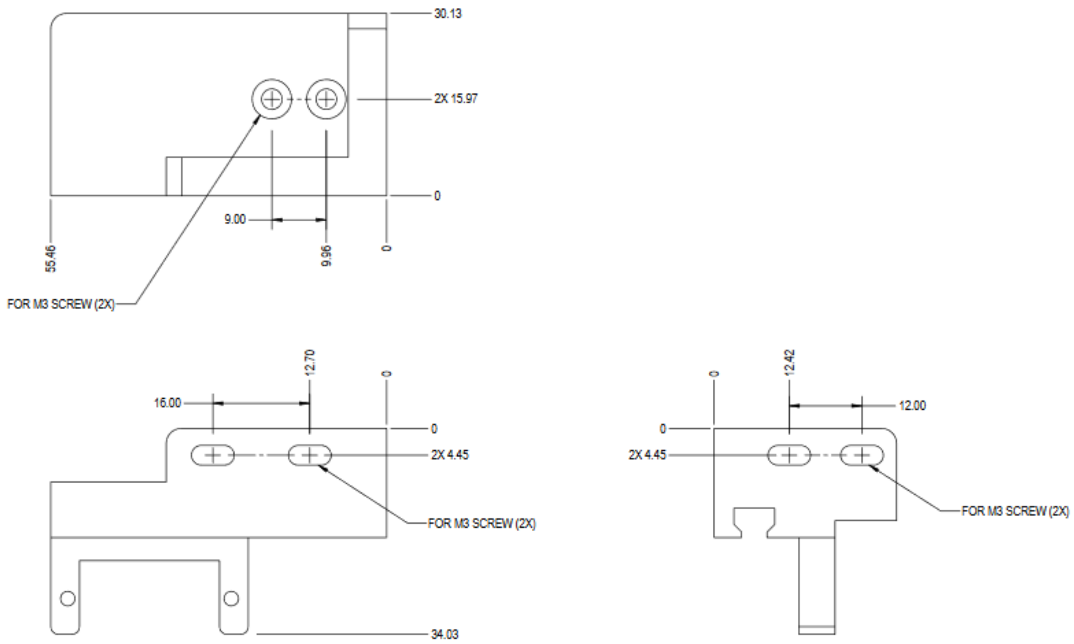

Figure 68 - Servo bracket measurements

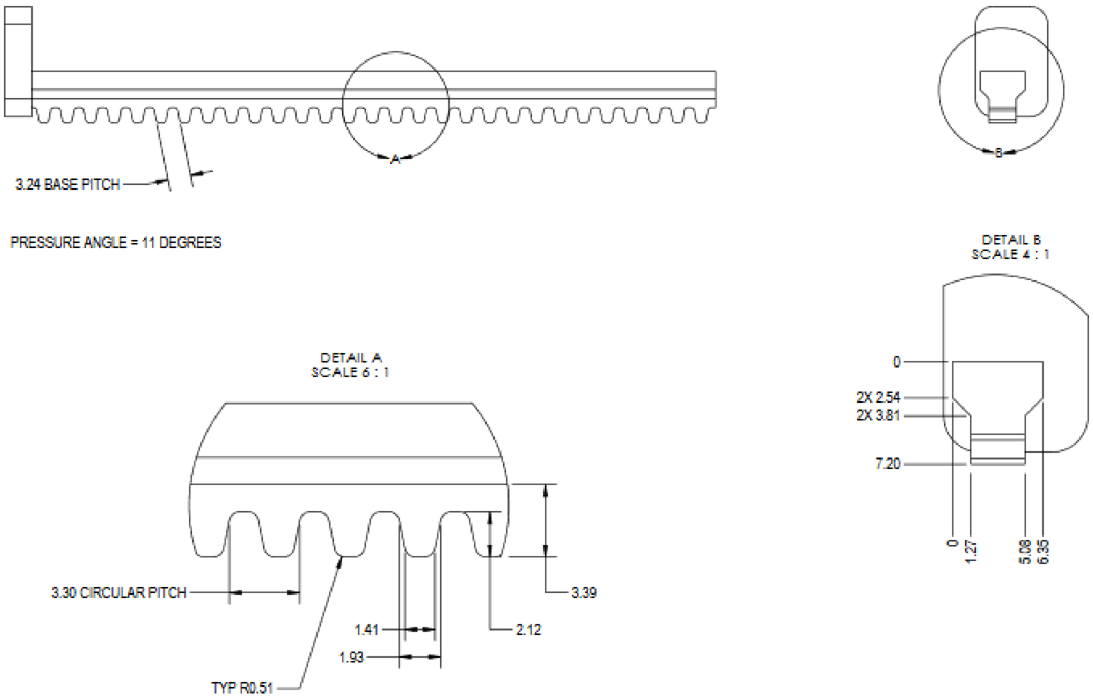

Figure 69 - Rack or pusher design and measurements